# An Experimental Study on the Generation and Growth of Wind Waves

AUTHOR(S):

KUNISHI, Hideaki

CITATION:

KUNISHI, Hideaki. An Experimental Study on the Generation and Growth of Wind Waves. Bulletins - Disaster Prevention Research Institute, Kyoto University 1963, 61: 1-41

ISSUE DATE:

1963-03-20

URL:

http://hdl.handle.net/2433/123733

DISASTER PREVENTION RESEARCH INSTITUTE
BULLETIN No. 61 MARCH, 1963

# AN EXPERIMENTAL STUDY ON THE GENERATION AND GROWTH OF WIND WAVES

BY

HIDEAKI KUNISHI

KYOTO UNIVERSITY, KYOTO, JAPAN

DISASTER PREVENTION RESEARCH INSTITUTE
KYOTO UNIVERSITY
BULLETINS

Bulletin No. 61 March, 1963

# An Experimental Study on the Generation and Growth of Wind Waves

Hideaki KUNISHI

# An Experimental Study on the Generation and Growth of Wind Waves

Hideaki KUNISHI

Abstract: Physical processes on wind waves were studied in our wind-flume experiments. It was found that there are at least three regimes in the course of the generation and growth of wind waves. We call them initial tremor, initial wavelet, and sea wave in order of their appearance. The initial wavelet which is generated at $w_*H/\nu_a \simeq 0.3$ is recognized as a roughness element on the water surface, and turns into the sea wave at $w_*H/\nu_a \simeq 200$ which has a character similar to that of what is called 'sea' An empirical universal law of initial wavelet which was found in our experiments and some discussions on physical mechanism of the generation and development of wind waves are presented. The numerical value of 'friction factor' is also shown.

## 1. Introduction

Research on sea and swell has made remarkable progress during the past twenty years. As is well known, development of the moderm theory was originated by H. U. Sverdrup and W. H. Munk (1943, 1946, 1947). Since then, many experimental and theoretical works have been carried out.

In 1945~6 the study of wave spectra was commenced in Britain by G. E. R. Deacon (1949), N. F. Barber and F. Ursell (1948). G. Neumann (1952a, b) developed the theory of wave growth on a somewhat different basis from Sverdrup-Munk's. M. S. Longuet-Higgins (1952) succeeded in giving a theoretical interpretation to the statistical nature of ocean waves. W. J. Pierson, Jr. (1952) found a general mathematical expression describing the actual wavy sea surface in terms of wave spectra.

G. Neumann (1953b) proposed a theoretical wave spectrum on the basis of his observations, which was afterwards employed in the new methods for forecasting by W. J. Pierson, Jr., G. Neumann and R. W. James (1955). Several other theoretical wave spectra were also proposed by J. Darbyshire (1952, 1955, 1956), H. U. Roll and G. Fischer (1956), and C. L. Bretschneider

(1959), and their relative merits have been widely discussed. Recently O. M. Phillips (1958a) offered an important contribution on the high frequency range in a wave spectrum.

Thus our knowledge of ocean waves is now quite comprehensive and much more systematic, neverthless it cannot be regarded as sufficient. Especially the physical mechanism of the first formation of waves by wind cannot be regarded as known at all. In a sense, the problem is merely mathematical, but real progress may be possible only when the suitable simplifications are made, as has been pointed out by F. Ursell (1956). Suggestions on the proper simplifications should be searched for in careful experimental works. Several theoretical hypotheses on wave generation have been proposed up to the present. These may be classified into three groups.

The first group takes the position that waves are generated through instability of the air-water current system. The first work of this type of calculations was done by Lord Kelvin (1871), which is well known as Kelvin-Helmholz instability. W. H. Munk (1947) made use of it to explain the existence of critical wind speed at which the appearance of sea surface turns from smooth to rough. This transition, however, is quite a different matter from the initial formation of waves by wind. W Wüst (1949) made calculations of the boundary-layer instability on several assumed laminar air-water velocity fields. R. C. Lock (1954) treated the same problem strictly on a laminar velocity profile which was theoretically calculated. J. W. Miles (1957) treated the case of turbulent air flow having a logarithmic profile.

The second group is concerned with the sheltering effect of normal pressure exerted on the wave surface. This idea was originally introduced by H. Jeffreys (1925, 1926). Afterwards, the possibility of interpretation of the wave generation by this effect was denied by T. E. Stanton's (1932) and H. Motzfeld's (1937) solid model experiments. Neverthless, it is an excellent idea physically. G. Neumann (1953a) has surmised from some empirical evidence that the sheltering coefficient is not a constant, but inversely proportional to the wave steepness for younger waves, while J. Darbyshire (1952) has assumed it to be proportional to the steepness.

It may be worth noting that the sheltering effect is tide in with the instability calculations, as has been explicitly shown by J. W. Miles (1957). In reality, it was his primary aim to predict the sheltering coefficients for

prescribed spectral component waves from stability calculations on an assumed shear flow. It should be kept in mind that the first and the second points of view are not unrelated to each other.

The last group pursues the cause in the stochastic fluctuations of normal pressure, which are unaffected by waves in contrast to the second point of view. C. Eckart (1953) made the first attempt, considering an ensemble of gusts travelling with wind. It proved, however, insufficient to explain actual wave production. O. M. Phillips (1957) proposed the alternative in which turbulent pressure fluctuations travelling with the mean wind velocities at heights of the same order as their dimensions above the water surface were considered to be the effective forces, and his mechanism of wave generation was essentially a sort of resonance.

All of these theoretical treatments contain uncertainties for whch it would be difficult to provide an adequate 'a priori' justification. With this situation as for as theory is concerned, careful and accurate laboratory experiments and field observations have been urgently needed. Few works, however, are available for appreciating the initial formation of waves. At the present time what we can reliably depend on through works done by H. U. Roll (1951), and by G. H. Keulegan (1951) is that (1) a minimum wind velocity capable of raising well-defined waves — initial wavelet — does exist and it diminishes with increasing distance from the windward edge of a limited fetch, and (2) even below such a critical velocity there exists a certain type of wave motions — initial tremor. The minimum wind velocity for the generation of initial wavelets has been found to be about 2～3 m/sec in laboratory experiments which corresponds to a short fetch, and to be about 0.8～1.1 m/sec in open conditions which corresponds to a moderate fetch.

The author has been interested in these problems and has been engaged for several years in laboratory work to investigate the nature of wind-generated waves ; such investigations have been conducted under the direction of Prof. S. Hayami. This paper is a detailed report of our experiments and analyses.

## Legend

$x$ Horizontal coordinate
$z$ Vertical coordinate
$t$ Time
$F$ Length of fetch
$g$ Acceleration of gravity
$\rho_a$ Density of air
$\nu_a$ Kinematic viscosity of air
$\rho_w$ Density of water
$\mu_w$ Molecular viscosity of water
$\nu_w$ Kinematic viscosity of water
$S$ Surface tension of water
$W$ Wind velocity
$\overline{W}$ Uniform wind velocity at the entrance of experimental flume
$W_{0.1}$ Wind velocity at 10 cm above the water surface
$W_{10}$ Wind velocity at 10 m above the water surface
$U$ Horizontal velocity of wind-driven current
$\tau_0$ Tangential stress at water surface
$w_*$ Friction velocity of air
$z_0$ Roughness parameter
$k$ Roughness height
$H$ Average wave height
$T$ Average wave period
$L$ Wave length
$C$ Phase velocity of wave
$G$ Group velocity of wave
$\delta$ Steepness of wave $=H/L$
$\beta'$ Wave age $=C/w_*$
$\Delta p$ Normal pressure fluctuation
$s$ Sheltering coefficient
$\gamma^2$ Friction factor
$R_N$ Mean rate of energy transfer to wave due to normal wind pressure
$R_\mu$ Mean rate of energy dissipation due to molecular viscosity of water
$E$ Mean total energy of water per unit area

# 2. Apparatus

## 2.1. Wind flume

For our experimental work a wind flume which was set up in the Disaster Prevention Research Institute of Kyoto University in 1955 was used. This flume consists of two parts as is shown schematically in Fig. 1. The entrance

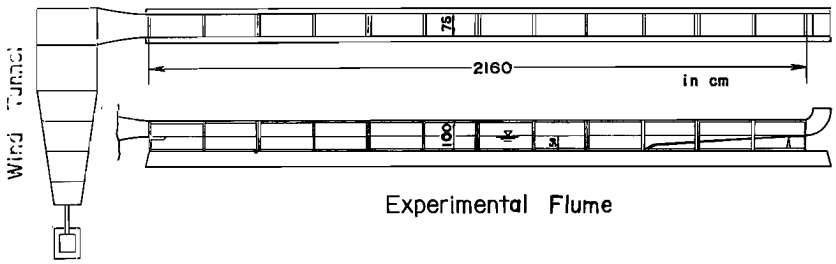


Fig. 1. Schematic view of wind flume.

assemblage is an ordinary wind tunnel from which uniform air flows are supplied to the experimental flume. The dimensions of the cross section of the downstream end, the opening of which is converged by the Venturi nozzle to about one fourth in area, are 50 cm in height and 75 cm in width. The closer inspections made in the preliminary tests for several wind velocities proved the uniformity of flows to be within $\pm 1\%$ up to 2 cm near walls. The wind velocity denoted $\overline{W}$, which is employed throughout this paper, means this uniform wind velocity. It can be continuously varied from abou 0.5 m/sec up to about 12 m/sec by means of changing the revolution speed of the blower. The blower is driven through a transmission by a constant speed motor of 5 h.p.. The experimental flume is a semi-closed conduit 21.6 m in length with a uniform rectangular cross section 100 cm deep and 75 cm wide. It consists of 12 sections constructed of steel with sides of glass. Its ceiling constructed of transparent plastic plates can be freely removed. The lower half of the flume is filled with water so that the depth of water is 50 cm and the air flows through the remaining upper half. At the upstream end of the flume a leading edge device is set up to make a smooth contact between air and water. In the downstream side of the flume a sloping floor made of steel with an angle of 3° is installed to prevent wave reflections. The air stream flows out upward through the end duct with a non-expanding cross section. The outward appearance of the experi-

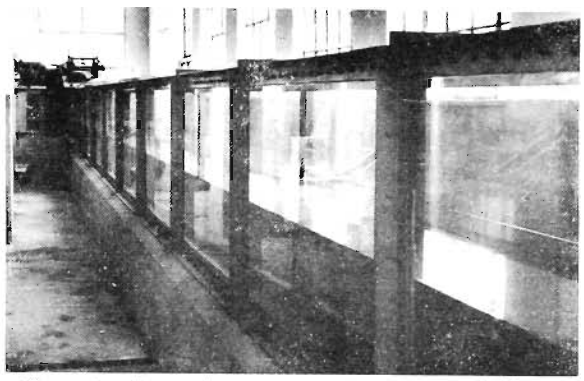

Photo. 1. Outward appearance of experimental flume.

mental flume is shown in Photo. 1.

Through numerous preliminary experiments carried out in 1957 it was found that the results from a tightly closed air passage were rather undesirable. In place of this the ceiling boards were adjusted case by case so that the velocity of the central part would not become too large along the wind passage in our experiments.

### 2.2. Measuring devices

To measure wind velocities a small cup-anemometer and a thermocouple anemometer were prepared for higher and lower velocities respectively. These are diagrammatically shown in Fig. 2 with their dimensions. The former is that which is used by micrometeorologist and the latter was devised by S. Kawata, et al. (1952).

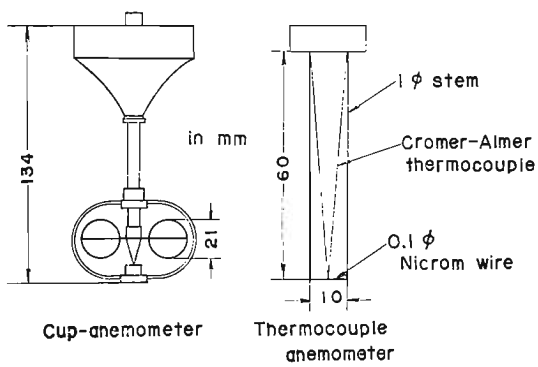


Fig. 2. Anemometers used in our experiments.

With the former being connected to a counter of electric contacts and the latter to an electronic recorder of full scale of 10 mV, these were carefully calibrated with the measurements by Pitot tube and by pursuing the smoke inserted in the stream. Obtained calibration formulae were as follows :

$$W=0.01+8.47N+0.030(N-0.073)^{-1} \quad \text{for} \quad N>0.15 \quad \cdots\cdots\cdots(2.1)$$

for the former and

$$1/E=0.090+0.255\sqrt{W} \quad \cdots\cdots\cdots\cdots\cdots(2.2)$$

for the latter, where $W$ is the mean wind velocity in m/sec, $N$ the number of electric contacts per second, and $E$ the electromotive force of thermocouple in mV The current supplied to the heating wire of thermocouple anemometer was 400 mA.

The cup-anemometer was useful for the velocities higher than 1.65 m/sec which corresponds to $N=0.15$. On the other hand, the thermocouple anemometer could be used successfully for the velocities lower than 3 m/sec, which overlap the former. The accuracy of measurements was estimated to be within about $\pm 1\%$ throughout the course of the experiment, with the exception of the region of 1~3 m/sec in the thermocouple anemometer, where the accuracy seemed to decrease gradually from $\pm 1\%$ to $\pm 2\%$. No measurements were available for the smallest velocities, below about 10 cm/sec, owing to the convection induced.

The resistive wave meter was used to measure the fluctuating interface between air and water, its sensor being shown schematically in Fig. 3 with its dimensions. Two measuring circuits shown in Fig. 4 were needed to learn the nature of the wind-generated waves through the whole range

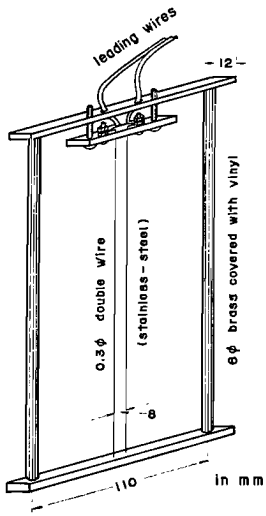


Fig. 3. Sensor of wave meter.

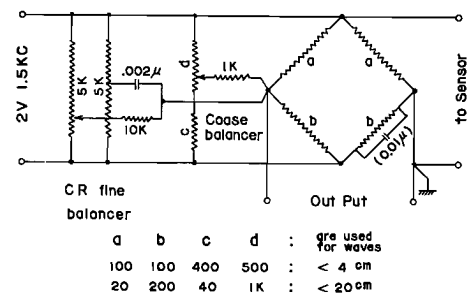


Fig. 4. Measuring circuits of wave meter.

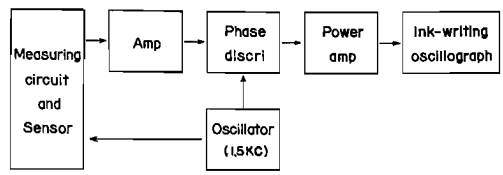


Fig. 5. Block diagram of wave meter.

of their growth. One circuit was designed to enable the magnification of the actual wave height from 1 to 20 times, and the other from 0.2 to 4 times, when they were connected to an ink-writing oscillograph through an amplifier. The amplifier used has the same construction as the strain meter commonly used, as can be seen from the block diagram shown in Fig. 5. The statical tests proved its accuracy to be within $\pm 1\%$. Since its gain depends upon the electric resistance of water which in turn depends on temperature, impurities, ete., frequent calibration is necessary for accurate measurements. In our experiments this calibration was performed prior to every run. It may be noted that a measuring circuit which would have been able to magnify as much as 100 times was also developed, but tests proved it to be unstable owing to the surface tension of water.

A device was also prepared to measure wave length. No more mention, however, will be made about it since the data obtained with it will not be used in this paper.

Fine alluminum powders dispersed uniformly in the water were used to obtain the current profiles induced in water by wind. It was needed that they were first wetted with alchol to allow dispersal in the water without lumping.

## 3. Measurement

### 3.1. Introductory remarks

Through preliminary visual observations it has been clearly recognized that a sudden growth of well-defined waves does exist in both fetch length and duration time, though there exists a certain type of waves before they start.

Concerning the steady state, the results of our observations are almost the same as G. H. Keulegan (1951) described in his paper. At very low wind velocities, say 50 cm/sec, the surface of the water remains almost calm everywhere. With an increase of the wind velocity, say at 1 m/sec, a certain type of wave motions becomes visible over whole fetches with suitable lighting. But these waves are too weak and vague to be considered as the so-called wind waves, although they seem to become somewhat vivid and definite on increasing the wind velocity. As a whole, the water surface in this condition is felt to be on a tension with a tremble. The

tension is strengthened with the wind speed until finally the sudden change in the appearance of the water surface occurs. When this sudden change occurs, the tension is immediately broken. In this sense we may call this type of wave 'initial tremor'. The term 'tremor' has been used by Keulegan. Somewhat detailed descriptions on the nature of this type of wave have been given in papers of H. U. Roll (1951) and W. G. van Dorn (1953). We can not, however, critically discuss them since our present experimental techniques are not suitable to measure them.

The sudden change in the appearance of the water surface begins to appear in the leeward part of the flume with the increase of wind velocity, and the windward part remains in the state of initial tremor. This leeward region is covered with definite wavelets whose length and height near the front of this region are estimated to be about 4 cm and 1 mm respectively. On further increasing the wind velocity the front edge of the wave region moves rather quickly to windward, so that soon after almost the entire water surface becomes covered with this type of wave. We should like to name this type of well-defined wave 'initial wavelet' It is our main purpose to make an investigation about this type of wave.

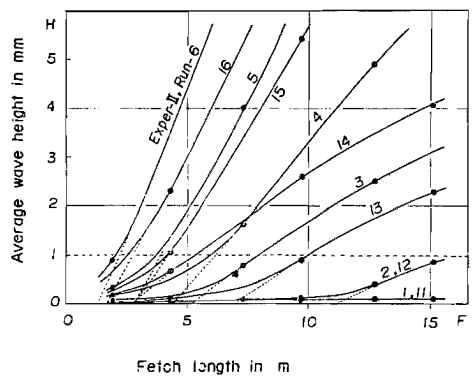


Fig. 6. Progression of the region of initial wavelet.

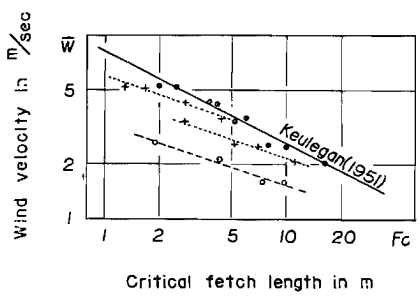


Fig. 7. Dependence of the critical fetch length on the wind velocity.

Fig. 6 shows the progression of the front of the region of initial wavelet with the wind velocity. The wind velocities $\overline{W}$ corresponding to run numbers 2 and 12, 14, 4, and 6 are about 2.1, 3.4, 3.6 and 5.2 m/sec respectively. When we define the position of the front as the fetch length where the average wave height is 1 mm, these critical lengths for various wind velocities are well in agreement with

Keulegan's observation, It is shown by solid circles and a full line in Fig. 7. The critical fetch length seems to be inversely proportional to the square of the wind velocity. But when we define the front edge as the point at which a naturally extended curve of average wave height against fetch (as is shown by dotted line in Fig. 6) intersects with the abscissa, these edge points lie on two lines different from Keulegan's. It is shown by cross marks and two dotted lines in Fig. 7. The separation of the observed points into two groups corresponds to the change of type of curve of the average wave height against fetch which occurs at the wind velocity of about 3.5 m/sec, as can be seen in Fig. 6. The critical fetch length is inversely proportional to the third power of the wind velocity. The blank circles in Fig. 7 correspond to the generation of initial wavelet which will be discussed later. They seem again to be inversely proportional to the third power of the wind velocity, as shown by a broken line in Fig. 7. Here the average wave height is only about 0.05 mm.

Similar processes can also be seen with respect to duration time.

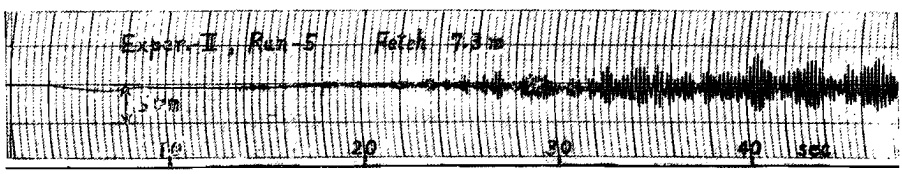


Photo. 2. A wave record showing the abrupt generation of inital wavelet.

In the lowest wind velocity, however long the wind might blow, the water surface remains calm, or in the state of initial tremor at most. With an increase of the wind velocity it is observed that the initial wavelets start suddenly and begin to grow quickly some time after the sudden onset of wind. Photo. 2 is an example of the wave records where such sudden generation and growth of the initial wavelets are obviously seen. The

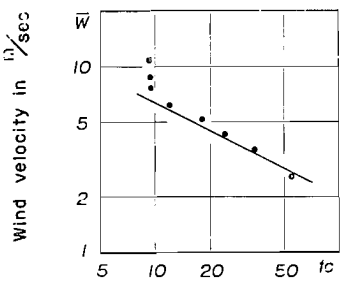


Fig. 8. Dependence of the critical duration time on the wind velocity.

critical duration time capable of generating the initial wavelets decreases with increasing wind velocity, and its dependence on the fetch seems rather little. Assuming that the average wave height at the critical time is 1 mm, we can find from the wave records that it is again inversely proportional to the square of the wind velocity, as is shown in Fig. 8. This is, however, not very reliable because of the difficulty in definitely ascertaining the average wave height near the critical time.

Setting aside minute discussions, there is no doubt as to the fact that the well-defined initial wavelets become rather suddenly visible to the naked eye. It should not be supposed that they are a simple continuation of the initial tremor. To elucidate this situation of wave generation, two series of experiments were carried out. They will be reported in the following sections.

### 3.2. Experiment at lower wind sppeeds

In the first experiment at low wind speeds, ranging from 0.5 to 2.3 m/sec, carried out in the autumn of 1957, the profile of the wind velocity above the water surface and of the very thin wind-driven currents near the surface were observed at a fetch of 7.9 m. Runs 1 to 11 were concerned with the former and 12 to 17 the latter. The wave meter was used only as an auxiliary, for initial wavelets were almost entirely absent in this experiment.

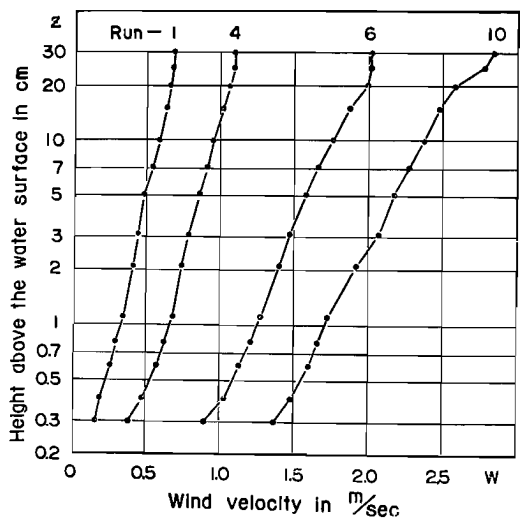


Fig. 9. Wwind profiles in the first experiment.

Each observation of the wind profile consists of measurements by the thermocouple anemometer of the wind velocities at fourteen heights above the water suface, ranging from 3 mm to 30 cm. Some examples are presented in Fig. 9, ordinate being the height above the surface on a logarithmic

scale and abscissa the wind velocity on a linear scale.

These profiles have a relatively good linear part in the range of height between 1 and 10 cm. Closer inspection has shown that the behaviour of this part of the profile can be compared to that of the well-known formula for the turbulent flow over smooth surfaces

$$\frac{W}{w_*}=5.75\log\frac{w_* z}{\nu_a}+5.5. \qquad \cdots\cdots\cdots\cdots\cdots\cdots(3.1)$$

From this point of view the friction velocity $w_*$ has been estimated for each run from the slope of the profile, taking the family of curves (3.1) with a parameter $w_*$ as a guide. The value of $\nu_a$ has been taken to be 0.151 cm²/sec corresponding to the mean temperature of 20.0°C during the period of experiment. The estimated values are tabulated in column 5 of Table 2. Using these values, we are able to summarize our data in a non-dimensional form. This will show how similar our profiles are to that of the turbulent flow over smooth surfaces. This will be discussed in Section 4.1.

The roughness parameter $z_0$ which is found in another more general formula for the turbulent flow i.e.

$$\frac{W}{w_*}=5.75\log\frac{z}{z_0} \qquad \cdots\cdots\cdots\cdots\cdots\cdots(3.2)$$

has been also determined for each run. These values are shown in column 6 of Table 2. In column 7 the corresponding values of the average wave height are also shown, although they are only rough estimates obtained from auxiliary wave records.

At the same time, the observation of drift current was made at the six wind velocities shown in Table 1. Each observation consists of tracing the

Table 1.

| Run No. | 12 | 13 | 14 | 15 | 16 | 17 |
|---|---|---|---|---|---|---|
| $\overline{W}$ m/sec | 0.48 | 0.62 | 0.81 | 0.94 | 1.40 | 2.08 |
| $W_{0.1}$ m/sec | 0.47 | 0.63 | 0.85 | 1.00 | 1.52 | 2.38 |
| $10^2\tau_0$ dynes/cm² Wind | 0.667 | 1.17 | 2.06 | 2.66 | 5.80 | 14.6 |
| derived from Water current | 0.640 | 1.18 | 2.08 | 2.61 | 5.60 | 12.7 |

loci of aluminium pewders on photographs taken at predetermined intervals of time in the course of development of the current. An example of these is given in Photo. 3, in which the white loci represent the velocities at various depths. As can be observed, the current is limited to a very thin layer.

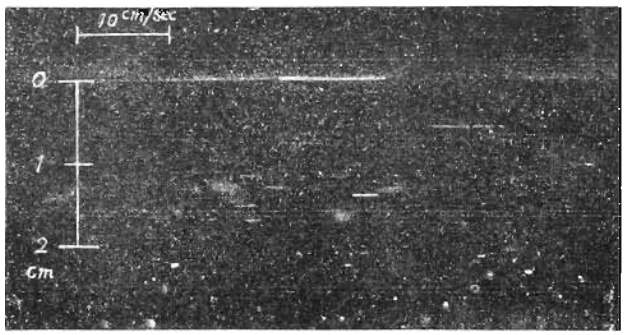


Photo. 3. A photograph showing a thin drift current induced by weak wind.

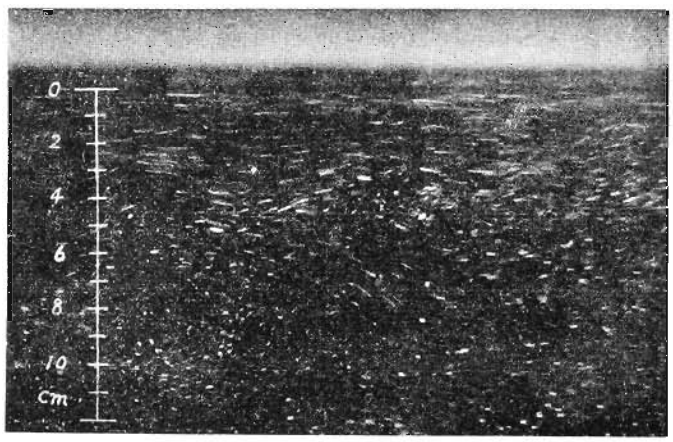


Photo. 4. Steady state of drift current.

As the wind commences to blow, this very thin current beings and starts to grow. Its velocity and thickness slowly increase until a steady state is attained. It is interesting to note that in all of our experimental runs the steady state was rather suddenly reached, always accompanied by eddies of a somewhat large scale. Photo. 4 illustrates this steady state.

From the data of the transient state of each run, the shearing stress at the water surface by wind and the kinematic viscosity of water has been

evaluated by the following formula, which is theoretically derived from the assumptions of a horizontal current in an infinitely deep water and of constant viscosity,

$$\left.\begin{aligned} U/U_0 &= e^{-\xi^2} - \sqrt{\pi}\,\xi\{1-\Phi(\xi)\}, \\ \text{where} \quad U_0 &= \frac{2}{\sqrt{\pi}}\frac{\tau_0}{\rho_w}\sqrt{\frac{t}{\nu_w}}, \quad \xi = \frac{z}{2\sqrt{\nu_w t}}, \end{aligned}\right\} \qquad \cdots\cdots\cdots\cdots(3.3)$$

where $z$ is the depth—positive downward from the surface, and $\Phi$ the error function. The suffix 0 means the surface value.

The viscosity was found to be the molecular one throughout our six runs with the exception of the data obtained after some time had elapsed in runs 18 to 20. The numerical value of molecular viscosity corresponding to the mean water temperature of 19.2°C during the period of this experiment is $1.04\times10^{-2}$ cm²/sec. The ascertained values of the surface stress for each run are shown in the last row of Table 1. From these results we obtained the non-dimensional current profile shown in Fig. 10. The abscissa and ordinate are proportional to $U/U_0$ and $\xi$ respectively and the full line represents the theoretical curve (3.3). The agreement between the observation and the theory indicates that this thin wind-driven current in transient state is a laminar flow and that our evaluation of surface stress is correct. More information about this current was obtained, but it will not be presented here in order not to digress from our present subject. Detailed discription has been given in another paper by the author (1957).

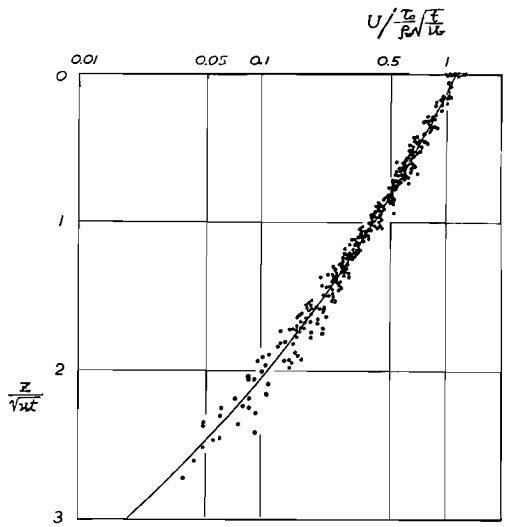


Fig. 10. Profile of drift current in non-dimensional form.

The fourth row of Table 1 is the surface stress derived from the wind observations. They have been estimated from the interpolation of the re-

sults of runs 1 to 11, using the relation

$$w_*^2 = \tau_0/\rho_a, \qquad \cdots\cdots\cdots\cdots\cdots\cdots(3.4)$$

where the density of air $\rho_a$ has been taken to be $1.22\times10^{-3}$ gr/cm$^3$. The agreement of these values of surface stress with those obtained from the current profile of water lead us to believe that our estimation of friction velocity derived from the observation of wind profile is also correct.

### 3.3. Experiment at higher wind speeds

The second experiment at higher wind speeds, ranging from 1.6 to 11 m/sec was performed in the fall of 1958. The profiles of the wind velocity above the mean water surface were observed at six fetches and wave records were taken simultaneously. Runs 1 to 10 were made at a set of fetches of 1.9, 7.3 and 12.7 m, and runs 11 to 20 at the other set of 4.3, 9.7 and 15.1 m.

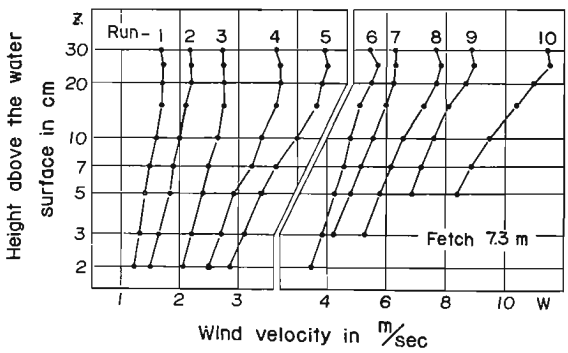


Fig. 11. Winds profiles in the second experiment.

The observations of the wind profile were made in the same manner as in the first experiment except that the cup-anemometer was pricipally used. Some examples are shown in Fig. 11. Good logarithmic behaviour is seen only at the lower part of the profiles—below 10 cm—in the same as in the first experiment. They are, however, so different from the formula (3.1) that the friction velociy $w_*$ and the roughness parameter $z_0$ have been determined by the method of least square for each run without any other guide. Some uncertainty of values (especially about $z_0$) could not

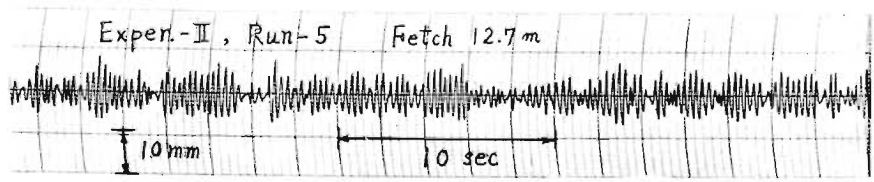


Photo. 5. A wave record in the steady state of waves.

Table 2.

| | 1 | 2 | 3 | 4 | 5 | 6 | 7 | 8 | 9 | 10 |
|---|---|---|---|---|---|---|---|---|---|---|
| | Run No. | $F$ m | $W$ m/sec | $W_{0.1}$ m/sec | $w_*$ cm/sec | $z_0$ mm | $H$ mm | $T$ sec | $L$ cm | $C$ cm/sec |
| Exper.-I | 1 | 7.9 | 0.50 | 0.49 | 2.42 | 0.0589 | — | | | |
| | 2 | 〃 | 0.58 | 0.59 | 2.86 | 0.0595 | (0.01) | | | |
| | 3 | 〃 | 0.72 | 0.74 | 3.56 | 0.0464 | (0.02) | | | |
| | 4 | 〃 | 0.94 | 0.95 | 4.79 | 0.0377 | (0.03) | | | |
| | 5 | 〃 | 1.10 | 1.18 | 5.70 | 0.0329 | — | | | |
| | 6 | 〃 | 1.60 | 1.76 | 8.26 | 0.0223 | (0.035) | | | |
| | 7 | 〃 | 1.76 | 1.93 | 8.85 | 0.0211 | (0.04) | | | |
| | 8 | 〃 | 1.88 | 2.12 | 9.70 | 0.0193 | (0.05) | | | |
| | 9 | 〃 | 1.96 | 2.17 | 10.3 | 0.0210 | (0.06) | | | |
| | 10 | 〃 | 2.06 | 2.37 | 11.2 | 0.0215 | (0.14) | | | |
| | 11 | 〃 | 2.28 | 2.62 | 12.2 | 0.0193 | (0.48) | | | |
| Exper.-II | | 1.9 | | 1.67 | 8.20 | 0.0199 | 0.0275 | 0.132 | 3.40 | 26.0 |
| | 1 | 7.3 | 1.64 | 1.59 | 7.83 | 0.0359 | 0.0688 | 0.187 | 5.90 | 30.9 |
| | | 12.7 | | 1.64 | 7.74 | 0.0247 | 0.0957 | 0.176 | 5.35 | 30.4 |
| | | 1.9 | | 2.09 | 10.3 | 0.0189 | 0.0415 | 0.148 | 4.05 | 27.4 |
| | 2 | 7.3 | 2.08 | 2.00 | 10.4 | 0.0501 | 0.107 | 0.155 | 4.42 | 28.5 |
| | | 12.7 | | 2.04 | 11.3 | 0.0794 | 0.410 | 0.135 | 3.52 | 26.1 |
| | | 1.9 | | 2.60 | 12.1 | 0.0135 | 0.0420 | 0.125 | 3.15 | 25.2 |
| | 3 | 7.3 | 2.57 | 2.64 | 14.3 | 0.0638 | 0.794 | 0.142 | 3.80 | 26.8 |
| | | 12.7 | | 2.44 | 14.3 | 0.118 | 2.52 | 0.207 | 7.02 | 33.9 |
| | | 1.9 | | 3.51 | 16.4 | 0.0199 | 0.182 | 0.095 | 2.21 | 23.2 |
| | 4 | 7.3 | 3.49 | 3.37 | 20.6 | 0.154 | 1.63 | 0.167 | 4.88 | 29.2 |
| | | 12.7 | | 3.12 | 19.1 | 0.162 | 4.92 | 0.224 | 8.13 | 36.3 |
| | | 1.9 | | 4.22 | 22.6 | 0.0548 | 0.317 | 0.076 | 1.77 | 23.0 |
| | 5 | 7.3 | 4.28 | 3.97 | 25.2 | 0.221 | 4.02 | 0.182 | 5.65 | 31.0 |
| | | 12.7 | | 3.98 | 27.1 | 0.336 | 8.56 | 0.272 | 11.8 | 43.4 |
| | | 1.9 | | 5.20 | 34.1 | 0.222 | 0.898 | 0.106 | 2.54 | 24.0 |
| | 6 | 7.3 | 5.19 | 4.76 | 35.1 | 0.411 | 7.70 | 0.228 | 8.50 | 37.3 |
| | | 12.7 | | 4.70 | 34.8 | 0.471 | 12.7 | 0.311 | 15.5 | 49.8 |
| | | 1.9 | | 6.05 | 43.2 | 0.364 | 2.56 | 0.121 | 3.00 | 25.0 |
| | 7 | 7.3 | 6.05 | 5.56 | 44.4 | 0.666 | 8.51 | 0.253 | 10.35 | 40.8 |
| | | 12.7 | | 5.20 | 37.0 | 0.366 | 16.8 | 0.370 | 21.7 | 58.6 |
| | | 1.9 | | 7.60 | 50.1 | 0.229 | 5.03 | 0.160 | 4.60 | 28.7 |
| | 8 | 7.3 | 7.50 | 6.55 | 47.8 | 0.404 | 11.4 | 0.293 | 13.65 | 46.6 |
| | | 12.7 | | 6.51 | 46.6 | 0.376 | 18.5 | 0.426 | 28.4 | 66.6 |

Table 2 (Continued).

| | 1 | 2 | 3 | 4 | 5 | 6 | 7 | 8 | 9 | 10 |
|---|---|---|---|---|---|---|---|---|---|---|
| Exper.-II | 9 | 1.9 | 8.67 | 8.75 | 66.6 | 0.519 | 5.37 | 0.235 | 9.00 | 38.3 |
| | | 7.3 | | 7.57 | 59.8 | 0.618 | 12.8 | 0.328 | 17.3 | 52.6 |
| | | 12.7 | | 7.36 | 60.2 | 0.694 | 26.5 | 0.410 | 26.3 | 64.2 |
| | 10 | 1.9 | 11.00 | 11.06 | 101.0 | 1.268 | 7.59 | 0.235 | 9.00 | 38.3 |
| | | 7.3 | | 9.44 | 79.1 | 0.785 | 22.5 | 0.376 | 22.4 | 59.5 |
| | | 12.7 | | 9.84 | 97.5 | 1.694 | 43.4 | 0.510 | 40.4 | 79.3 |
| | 11 | 4.3 | 1.55 | 1.75 | 8.18 | 0.0236 | 0.0248 | 0.197 | 6.50 | 33.0 |
| | | 9.7 | | 1.57 | 7.70 | 0.0296 | 0.0615 | 0.203 | 6.83 | 33.7 |
| | | 15.1 | | 1.33 | 6.78 | 0.0401 | 0.0945 | 0.189 | 6.05 | 32.0 |
| | 12 | 4.3 | 2.02 | 2.12 | 10.5 | 0.0296 | 0.0425 | 0.133 | 3.48 | 26.0 |
| | | 9.7 | | 2.02 | 9.74 | 0.0252 | 0.126 | 0.144 | 3.90 | 27.0 |
| | | 15.1 | | 1.78 | 9.83 | 0.0781 | 0.843 | 0.146 | 4.00 | 27.2 |
| | 13 | 4.3 | 2.53 | 2.69 | 12.9 | 0.0232 | 0.107 | 0.123 | 3.09 | 25.1 |
| | | 9.7 | | 2.48 | 14.8 | 0.124 | 0.915 | 0.132 | 3.42 | 25.9 |
| | | 15.1 | | 2.10 | 12.4 | 0.119 | 2.29 | 0.173 | 5.19 | 30.0 |
| | 14 | 4.3 | 3.45 | 3.65 | 23.7 | 0.222 | 0.684 | 0.120 | 3.00 | 25.0 |
| | | 9.7 | | 3.22 | 20.9 | 0.211 | 2.59 | 0.193 | 6.24 | 32.3 |
| | | 15.1 | | 2.73 | 17.6 | 0.217 | 4.04 | 0.237 | 9.08 | 38.3 |
| | 15 | 4.3 | 4.23 | 4.38 | 28.4 | 0.237 | 1.04 | 0.118 | 2.90 | 24.6 |
| | | 9.7 | | 3.66 | 25.3 | 0.345 | 5.41 | 0.224 | 8.13 | 36.3 |
| | | 15.1 | | 3.67 | 24.4 | 0.251 | 12.5 | 0.306 | 15.0 | 48.8 |
| | 16 | 4.3 | 5.10 | 5.25 | 39.7 | 0.480 | 2.30 | 0.143 | 3.82 | 26.7 |
| | | 9.7 | | 4.86 | 36.2 | 0.504 | 9.24 | 0.255 | 10.45 | 41.0 |
| | | 15.1 | | 4.45 | 33.2 | 0.474 | 15.3 | 0.350 | 19.3 | 55.3 |
| | 17 | 4.3 | 6.00 | 5.82 | 43.5 | 0.501 | 7.20 | 0.194 | 6.29 | 32.4 |
| | | 9.7 | | 5.68 | 46.3 | 0.745 | 9.69 | 0.289 | 13.3 | 46.0 |
| | | 15.1 | | 5.10 | 37.4 | 0.398 | 19.0 | 0.390 | 24.0 | 61.7 |
| | 18 | 4.3 | 7.35 | 6.80 | 52.8 | 0.562 | 7.44 | 0.244 | 9.61 | 39.4 |
| | | 9.7 | | 6.59 | 47.6 | 0.377 | 18.4 | 0.337 | 18.0 | 53.5 |
| | | 15.1 | | 6.60 | 45.9 | 0.322 | 24.0 | 0.455 | 32.6 | 71.6 |
| | 19 | 4.3 | 8.62 | 7.94 | 73.7 | 1.340 | 9.18 | 0.253 | 10.35 | 41.0 |
| | | 9.7 | | 7.59 | 57.7 | 0.536 | 20.3 | 0.389 | 24.0 | 61.8 |
| | | 15.1 | | 7.28 | 59.8 | 0.696 | 30.4 | 0.440 | 30.1 | 68.5 |
| | 20 | 4.3 | 10.93 | 10.04 | 97.6 | 1.761 | 13.0 | 0.300 | 14.4 | 48.0 |
| | | 9.7 | | 9.77 | 100.5 | 1.993 | 27.8 | 0.455 | 32.6 | 71.6 |
| | | 15.1 | | 9.90 | 97.9 | 1.717 | 36.4 | 0.578 | 52.0 | 90.0 |

Table 3.

| 1 | 2 | 3 | 4 | 5 | 6 | 7 | 8 | 9 | 10 | 11 | 12 |
|---|---|---|---|---|---|---|---|---|---|---|---|
| Run No. | $F$ m | $\beta'$ | $10^2\delta$ | $\frac{w_* z_0}{\nu_\alpha}$ | $\frac{w_* H}{\nu_\alpha}$ | $10^{-2}\frac{w_* L}{\nu_\alpha}$ | $10^{-2}\frac{gF}{w_*^2}$ | $10^2\frac{gz_0}{w_*^2}$ | $10^2\frac{gH}{w_*^2}$ | $W_{10}$ m/sec | $10^3\gamma^2$ |
| | 1.9 | 3.18 | 0.081 | 0.109 | 0.150 | 1.86 | 27.7 | 2.90 | 4.08 | 2.69 | 0.93 |
| 1 | 7.3 | 3.95 | 0.117 | 0.187 | 0.359 | 3.08 | 117 | 5.73 | 11.0 | 2.45 | 1.02 |
| | 12.7 | 3.93 | 0.181 | 0.127 | 0.494 | 2.76 | 208 | 4.04 | 15.7 | 2.50 | 0.96 |
| | 1.9 | 2.66 | 0.103 | 0.130 | 0.285 | 2.78 | 17.6 | 1.75 | 3.83 | 3.39 | 0.92 |
| 2 | 7.3 | 2.74 | 0.242 | 0.347 | 0.742 | 3.06 | 66.1 | 4.54 | 9.69 | 3.17 | 1.08 |
| | 12.7 | 2.31 | 1.16 | 0.598 | 3.09 | 2.65 | 97.5 | 6.09 | 31.5 | 3.31 | 1.16 |
| | 1.9 | 2.08 | 0.133 | 0.109 | 0.339 | 2.54 | 12.7 | 0.904 | 2.81 | 4.08 | 0.88 |
| 3 | 7.3 | 1.87 | 2.09 | 0.608 | 7.57 | 3.62 | 35.0 | 3.06 | 38.1 | 4.27 | 1.12 |
| | 12.7 | 2.37 | 3.58 | 1.12 | 24.0 | 6.69 | 60.9 | 5.66 | 121 | 4.05 | 1.25 |
| | 1.9 | 1.41 | 0.824 | 0.218 | 1.99 | 2.42 | 6.92 | 0.725 | 6.63 | 5.38 | 0.93 |
| 4 | 7.3 | 1.42 | 3.34 | 2.11 | 22.4 | 6.70 | 16.9 | 3.56 | 37.6 | 5.70 | 1.31 |
| | 12.7 | 1.90 | 6.05 | 2.06 | 62.6 | 10.4 | 34.1 | 4.35 | 132 | 5.26 | 1.32 |
| | 1.9 | 1.02 | 1.79 | 0.826 | 4.78 | 2.67 | 3.65 | 1.05 | 6.08 | 6.84 | 1.09 |
| 5 | 7.3 | 1.23 | 7.12 | 3.71 | 67.5 | 9.49 | 11.3 | 3.41 | 62.0 | 6.75 | 1.40 |
| | 12.7 | 1.60 | 7.25 | 6.07 | 155 | 21.3 | 17.0 | 4.48 | 114 | 6.97 | 1.51 |
| | 1.9 | 0.70 | 3.54 | 5.05 | 20.4 | 5.77 | 1.60 | 1.87 | 7.57 | 9.12 | 1.40 |
| 6 | 7.3 | 1.06 | 9.06 | 9.62 | 180 | 19.9 | 5.81 | 3.27 | 61.3 | 8.85 | 1.57 |
| | 12.7 | 1.43 | 8.17 | 10.9 | 295 | 36.0 | 10.3 | 3.81 | 103 | 8.66 | 1.62 |
| | 1.9 | 0.58 | 8.52 | 10.5 | 73.7 | 8.64 | 0.998 | 1.91 | 13.4 | 11.03 | 1.54 |
| 7 | 7.3 | 0.92 | 8.22 | 19.7 | 252 | 30.6 | 3.63 | 3.31 | 42.3 | 10.66 | 1.73 |
| | 12.7 | 1.58 | 7.72 | 9.03 | 414 | 53.5 | 9.09 | 2.62 | 120 | 9.44 | 1.54 |
| | 1.9 | 0.57 | 10.9 | 7.65 | 168 | 15.4 | 0.742 | 0.886 | 19.6 | 13.37 | 1.41 |
| 8 | 7.3 | 0.98 | 8.37 | 12.9 | 363 | 43.5 | 3.13 | 1.73 | 48.9 | 12.08 | 1.57 |
| | 12.7 | 1.43 | 6.53 | 11.7 | 575 | 88.2 | 5.73 | 1.70 | 83.5 | 11.86 | 1.54 |
| | 1.9 | 0.58 | 5.97 | 23.0 | 238 | 40.0 | 0.420 | 1.15 | 11.9 | 16.41 | 1.65 |
| 9 | 7.3 | 0.88 | 7.39 | 24.6 | 510 | 69.0 | 2.00 | 1.69 | 35.1 | 14.47 | 1.71 |
| | 12.7 | 1.07 | 10.1 | 27.9 | 1060 | 106 | 3.43 | 1.88 | 71.7 | 14.40 | 1.75 |
| | 1.9 | 0.38 | 8.44 | 85.4 | 511 | 60.6 | 0.183 | 1.22 | 7.92 | 22.63 | 1.99 |
| 10 | 7.3 | 0.75 | 10.0 | 41.4 | 1190 | 118 | 1.14 | 1.18 | 35.2 | 18.67 | 1.80 |
| | 12.7 | 0.81 | 10.7 | 100 | 2820 | 263 | 1.31 | 1.75 | 44.7 | 21.14 | 2.13 |
| | 4.3 | 4.04 | 0.038 | 0.129 | 0.135 | 3.55 | 63.0 | 3.46 | 3.63 | 2.65 | 0.96 |
| 11 | 9.7 | 4.38 | 0.090 | 0.152 | 0.316 | 3.51 | 160 | 4.89 | 10.2 | 2.45 | 0.99 |
| | 15.1 | 4.72 | 0.156 | 0.181 | 0.427 | 2.74 | 322 | 8.54 | 20.2 | 2.10 | 1.04 |

Table 3 (Continued).

| 1 | 2 | 3 | 4 | 5 | 6 | 7 | 8 | 9 | 10 | 11 | 12 |
|---|---|---|---|---|---|---|---|---|---|---|---|
| | 4.3 | 2.48 | 0.122 | 0.207 | 0.298 | 2.44 | 38.2 | 2.63 | 3.78 | 3.34 | 0.99 |
| 12 | 9.7 | 2.77 | 0.323 | 0.164 | 0.818 | 2.53 | 100 | 2.60 | 13.0 | 3.14 | 0.97 |
| | 15.1 | 2.77 | 2.10 | 0.512 | 5.52 | 2.62 | 153 | 7.92 | 85.5 | 2.89 | 1.16 |
| | 4.3 | 1.94 | 0.345 | 0.200 | 0.920 | 2.66 | 25.3 | 1.37 | 6.30 | 4.18 | 0.95 |
| 13 | 9.7 | 1.75 | 2.68 | 1.22 | 9.03 | 3.38 | 43.4 | 5.55 | 40.9 | 4.17 | 1.26 |
| | 15.1 | 2.42 | 4.41 | 0.984 | 18.9 | 4.29 | 96.2 | 7.58 | 146 | 3.51 | 1.25 |
| | 4.3 | 1.05 | 2.28 | 3.51 | 10.8 | 4.74 | 7.50 | 3.87 | 11.9 | 6,34 | 1.40 |
| 14 | 9.7 | 1.54 | 4.15 | 2.94 | 36.1 | 8.69 | 21.8 | 4.73 | 58.1 | 5.62 | 1.38 |
| | 15.1 | 2.18 | 4.45 | 2.55 | 47.4 | 10.7 | 47.8 | 6.86 | 128 | 4.72 | 1.39 |
| | 4.3 | 0.87 | 3.59 | 4.49 | 19.7 | 5.49 | 5.22 | 2.88 | 12.6 | 7.55 | 1.41 |
| 15 | 9.7 | 1.44 | 6.65 | 5.82 | 91.3 | 13.7 | 14.9 | 5.28 | 82.8 | 6.49 | 1.52 |
| | 15.1 | 2.00 | 8.33 | 4.08 | 203 | 24.4 | 24.9 | 4.13 | 206 | 6.45 | 1.43 |
| | 4.3 | 0.68 | 6.02 | 12.7 | 60.9 | 10.1 | 2.67 | 2.98 | 14.3 | 9.86 | 1.62 |
| 16 | 9.7 | 1.13 | 8.84 | 12.2 | 223 | 25.2 | 7.25 | 3.77 | 69.1 | 8.95 | 1.64 |
| | 15.1 | 1.67 | 7.92 | 10.5 | 339 | 42.7 | 13.4 | 4.21 | 136 | 8.26 | 1.62 |
| | 4.3 | 0.75 | 11.4 | 14.5 | 209 | 18.2 | 2.19 | 2.55 | 36.6 | 10.76 | 1.64 |
| 17 | 9.7 | 1.01 | 7.28 | 23.0 | 299 | 41.1 | 4.43 | 3.41 | 44.3 | 10.99 | 1.78 |
| | 15.1 | 1.65 | 7.93 | 9.92 | 474 | 59.8 | 10.6 | 2.79 | 133 | 9.46 | 1.56 |
| | 4.3 | 0.75 | 7.75 | 19.8 | 262 | 33.8 | 1.51 | 1.98 | 26.2 | 12.90 | 1.67 |
| 18 | 9.7 | 1.12 | 5.11 | 12.0 | 584 | 57.1 | 4.20 | 1.63 | 79.6 | 12.11 | 1.55 |
| | 15.1 | 1.56 | 3.69 | 9.85 | 734 | 99.8 | 7.02 | 1.50 | 112 | 11.86 | 1.50 |
| | 4.3 | 0.56 | 8.87 | 65.8 | 451 | 50.9 | 0.776 | 2.42 | 16.6 | 16.41 | 1.84 |
| 19 | 9.7 | 1.07 | 8.46 | 20.6 | 781 | 92.3 | 2.86 | 1.58 | 59.8 | 14.17 | 1.66 |
| | 15.1 | 1.15 | 10.1 | 27.8 | 1210 | 120 | 4.14 | 1.91 | 83.3 | 14.30 | 1.75 |
| | 4.3 | 0.49 | 9.01 | 115 | 846 | 93.7 | 0.442 | 1.81 | 13.4 | 21.07 | 2.15 |
| 20 | 9.7 | 0.71 | 8.53 | 134 | 1860 | 218 | 0.941 | 1.93 | 27.0 | 21.38 | 2.21 |
| | 15.1 | 0.92 | 7.00 | 112 | 2380 | 339 | 1.54 | 1.76 | 37.2 | 21.20 | 2.13 |

be avoided since the number of measuring heights was limited. The obtained values are tabulated in columns 5 and 6 of Table 2.

Each wave record consists of two parts. The first part is concerned with the transient state to find the initial epoch of the generation of initial wavelets. Its example is shown in Section 3. (Photo. 2), and a discussion is presented there. The second part has been taken in the steady state of waves to find some wave characteristics, with recording speed

being increased to 40 mm/sec. Photo. 5 is a typical wave record in the steady state of waves (recording speed : 5 mm/sec.). As can be observed, there are very noticable beats. From these records the average wave height $H$ and the average wave period $T$ of 50 or more successive individual waves have been determined for each run. The wave length $L$ and the phase velocity of wave $C$ have also been calculated graphically by the following formula for free surface waves in deep water

$$C^2=\frac{gL}{2\pi}+\frac{2\pi S}{\rho_w L} \quad \text{and} \quad L=CT. \qquad \cdots\cdots\cdots\cdots\cdots\cdots(3.5)$$

These are tabulated in columns 7 to 10 of Table 2. As is mentioned in Section 2.2, independent measurements of the wave length were also attempted. Though detailed analysis of these has not been made, a rough estimate of them seems to support the formula (3.5).

In Table 3, the values of various non-dimensional quantities which have been calculated from the values of Table 2, and will be used through Sections 4, are summarized. The kinematic viscosity of air $\nu_a$ has been taken to be 0.150 cm$^2$/sec corresponding to the mean air temperature of 19.0°C during the period of our second experiment.

## 4. Analysis and Discussion

### 4.1. Generation of initial wavelet and roughness of water surface

The non-dimensional profile of weak winds has shown to be of much value. This profile is shown in Fig. 12, in which are plotted 104 data obtained from measuring heights below 25 cm in runs 1 to 8. A height of 25 cm above the water surface is the centre of the wind passage in our experimental flume. Three runs have been omitted, since they differ slightly from the others.

Lline (A) in Fig. 12 represents the logarithmic formula (3.1), and cure (B) indicates what is called the laminar sub-layer. It has been established that an actual flow profile over a smooth surface begins to deviate gradually downwards from the line (A) near $w_* z/\nu_a=30$ and joins the curve (B) near $w_* z/\nu_a=8$. Our data also show the same general behaviour, and it seems sufficient to believe that our data obey the universal velocity distribution of the flow over smooth surfaces, although there are several

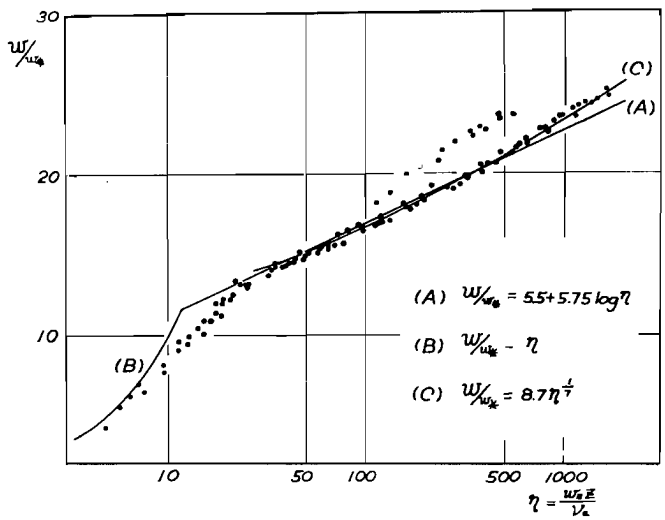


Fig. 12. Profile of weak winds in non-dimensional form.

data which differ from the others and our data deviate slightly upwards from the line (A) at the right.

In the same figure another expression of flow profile which is called the power law is also shown as curve (C)

$$\frac{W}{w_*} = 8.7\left(\frac{w_* z}{\nu_a}\right)^{1/7} \qquad \cdots\cdots\cdots\cdots\cdots\cdots (4.1)$$

Our data seem generally to follow (C) rather than (A). The fourteen data showing the marked upward departure are those obtained at the heights above 7 cm in runs 1 and 2, and above 10 cm in run 3. The causes of this departure are not clear. But, there seem to be no doubt that the weak wind above the water surface for which there is no initial wavelet is the turbulent flow over smooth surfaces. It is particularly important to note that it has a very thin laminar sub-layer.

The profile of the stronger wind, on the other hand, differs markedly from the one above. It should be regarded as the turbulent flow over rough surfaces. Fig. 13 shows the relation between the wind velocity at 10 cm above the water surface $W_{0.1}$ and the friction velocity $w_*$ at the fetches of 4.3 and 15.1 m (Exper. 2), and of 7.9 m (Exper. 1). $W_{0.1}$ is chosen as a representative wind velocity, since a height of 10 cm seems to be the upper limit of the good logarithmic part in wind profile through all

of our data. The full line indicates the relation of smooth surfaces which is calculated by the equation (4.1). On increasing the wind velocity the friction velocity or the surface stress begins to deviate from that of smooth surfaces at a certain critical wind velocity and such deviation becomes greater and greater. This means that the water surface changes from smooth to rough at a critical wind velocity and becomes more rough with the increase of wind velocity. It may be noted here that such critical wind velocities differ for the different fetches, as can be seen in

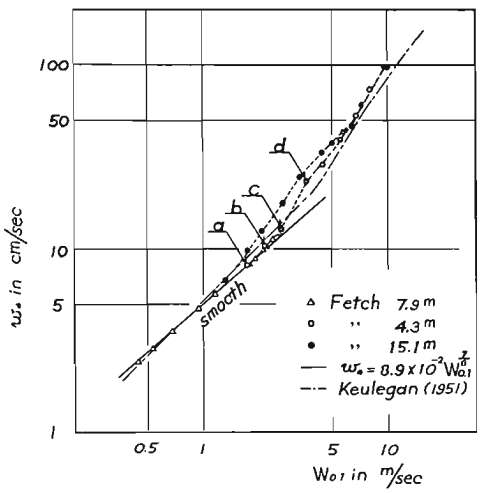


Fig. 13. Relation between friction velocity and wind velocity.

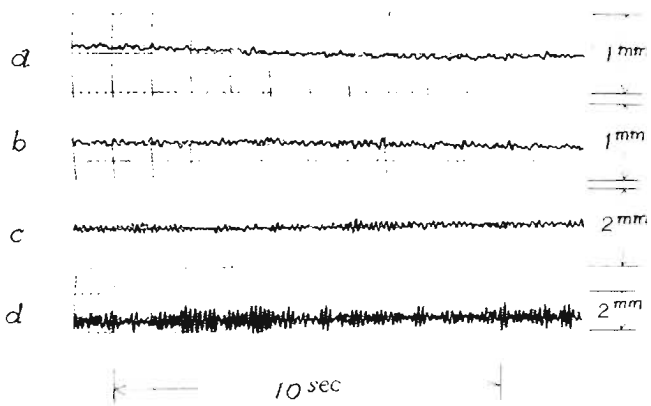


Photo. 6. Wave records showing the generation and development of initial wavelet.

Fig. 13.

Similar results have been obtained by G. H. Keulegan (1951) and W. G. van Dorn (1953) from observation of the surface slope generated by

wind, and interpreted as an additive stress due to the presence of waves. In Fig. 13 Keulegan's curve is shown by a chain line with one dot for comparison. Photo. 6 is a set of wave records at the fetch of 4.3 m. The letter affixed to each record corresponds to those in Fig. 13. In state 'a' where the friction velocity is still regarded as that of smooth surfaces, the waves seem to have no character of initial wavelets, but look somewhat like a white noise. Sstate 'b' is critical where the character of typical initial wavelets is first observed in places. This character with some beats is clearly seen in state 'c' and becomes more evident in state 'd'.

It is worth noting that the rather sudden increase of friction velocity or surface stress has an intimate relationship with the generation of initial wavelets and accordingly that the change of water surface from smooth to rough is intimately related with the generation of initial wavelets. From the first point of view, we can assert that the sudden increase of shearing stress at the water surface results not only from the presence of waves but rather from generating the initial wavelets. There is mutual action between the initial wavelet and the air flow, that is, the initial wavelets are generated and developed by the shearing stress and the shearing stress is in turn increased by the generation and development of initial wavelets The second point of view is more suggestive. It leads us to the idea that the initial wavelets are equivalent to the roughness elements.

The verification of this point of view comes from studying Fig. 14. The wind profile over rough surfaces is usually given by

$$\frac{W}{w_*}=5.75\log\frac{z}{k}+A_r\left(\frac{w_*k}{\nu_a}\right), \qquad \cdots\cdots\cdots\cdots\cdots(4.2)$$

where $k$ is called roughness height. $A_r$ is a function of $w_*k/\nu_a$ alone. If we transform this equation to the following expression

$$\frac{W}{w_*}=5.75\log\frac{w_*z}{\nu_a}+C_r\left(\frac{w_*k}{\nu_a}\right), \qquad \cdots\cdots\cdots\cdots\cdots(4.3)$$

it will be recognized that $C_r$ is also a function of $w_*k/\nu_a$ alone. The value of the quantity $C_r$ can be calculated from observations in the following ways, one being deduced readily from (4.3) and the other with the aid of (3.2),

$$C_r=\frac{W}{w_*}-5.75\log\frac{w_*z}{\nu_a}=-5.75\log\frac{w_*z_0}{\nu_a}, \quad \cdots\cdots\cdots\cdots(4.4)$$

because both right hand sides can be known by measurements.

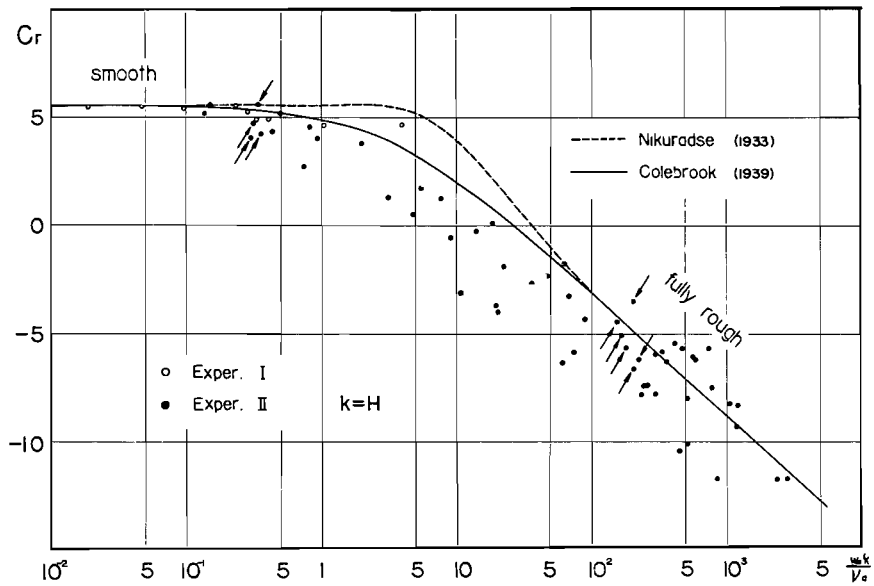


Fig. 14. Relation between $C_r$ and $w_*H/\nu_a$.

Assuming the average wave height $H$ as the roughness height $k$, we obtain Fig. 14 from all of our data. The broken line in this figure indicates the established result of J. Nikuradse (1933) for artificially sand roughned pipes and the full line that of C. F. Colebrook (1939) for commercial pipes. The former type of roughness is called the sand roughness and the latter the natural roughness. Though our data show a rather wide scattering, we find a definite trend similar to that of the natural roughness. This remarkable fact tells us that the average wave height may be considered the roughness height itself or at least the height proportional to it.

To further confirm this point Fig. 15 is presented. We may assume after Colebrook's work that the wind profile above the water surface —the surface with natural roughness— can be expressed by the following equation

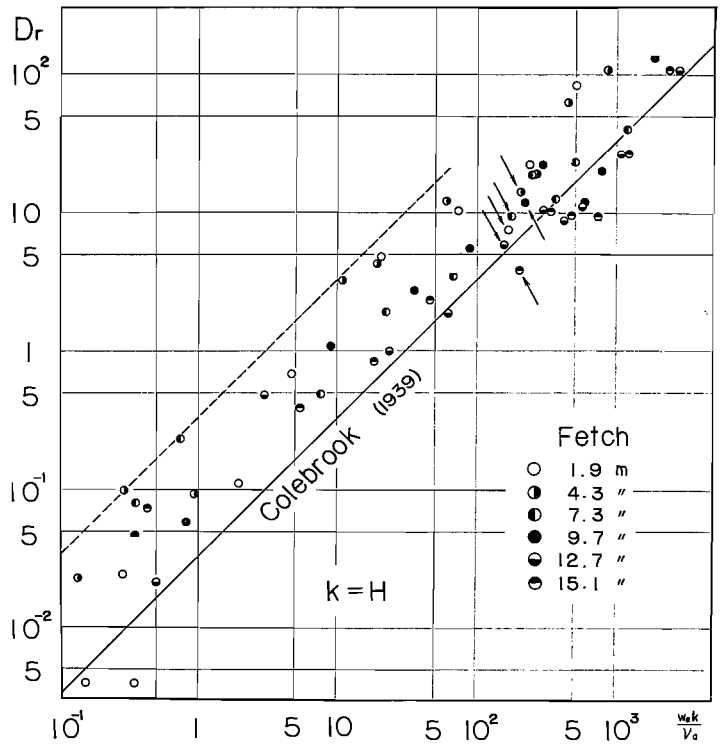


Fig. 15. Relation between $D_r$ and $w_*H/\nu_a$.

$$\frac{W}{w_*}=5.75\log\frac{z}{m\frac{\nu_a}{w_*}+nk}. \qquad \cdots\cdots(4.5)$$

where $m$ and $n$ are numerical constants. The value of $m$ proves to be $0.105\simeq 1/9$ by the formula (3.1), while $n$ may be considered to be of $0.0335\simeq 1/30$ in the case of the flow along solid walls, but it may not be so in other conditions. Indeed, W. Paeschke (1937) found its value 1/7 for surfaces covered with various kinds of vegetation. Now, comparing the above equation with the general formula (3.2), we can easily obtain the following expression

$$\frac{w_*z_0}{\nu_a}=m+n\frac{w_*k}{\nu_a}. \qquad \cdots\cdots(4.6)$$

If we assume here again that $k=H$, from observation we shall be able to estimate the value of $n$ for the wavy water surface. Calculating the values

of the following quantity

$$D_r=\frac{w_*z_0}{\nu_a}-m \qquad \cdots\cdots\cdots\cdots\cdots\cdots(4.7)$$

from all of our data in the second experiment and plotting them against $w_*H/\nu_a$, we obtain Fig. 15. Our data, which are shown here by the different marks indicating the different fetches, scatter almost uniformly within two lines, full and broken. The full line represents a naturally rough solid wall in which $n\simeq 1/30$, while the broken line $n=1/3$. Our data seem to depend slightly on the fetch, but this is not clear. Hence, we may state that the value of $n$ for the wavy water surface lies between 1/3 and 1/30 and its most probable value may be about 1/10. The value of 1/10 is comparable to Paeschker's value. Thus we can state that the initial wavelet is the roughness element itself.

From inspection of the wave records it is found that the critical wave states for the fetches of 1.9, 4.3, 7.3 and 9.7 m are seen on the data of runs 3, 12, 1 and 11 respectively. The values of $w_*H/\nu_a$ for these data all prove to be of nearly 0.3 as shown by arrows at the left part of Fig. 14. This also seems to support our conclusion. Because the quantity $w_*H/\nu_a$ represents the ratio of the average wave height to the thickness of the laminar sub-layer and the constancy of its value for the first formation of initial wavelets means that these wavelets are intimately related with the sub-layer and are generated in a definite manner. Thus, we can finally conclude that the initial wavelet is generated and developed as the roughness element itself and the critical number of its generation is $w_*H/\nu_a \simeq 0.3$. A rough estimate of the average wave height at the critical state is 0.05 mm.

O. Sibul (1955) has also conducted a measurement similar to ours in a laboratory wave channel to investigate the roughness of the water surface and the shearing stress exerted on the water surface by wind. In contrast to our results he concluded that there seems to be no relationship between wave height and the roughness parameter. Though the author can give no reason for this discrepancy, it is worth noting in Fig. 14 that half of his data are in agreement with ours, but the other half are widely scattered in the upper right part of the figure between the line indicating fully rough surfaces and the extension to right of the line indicating smooth surfaces.

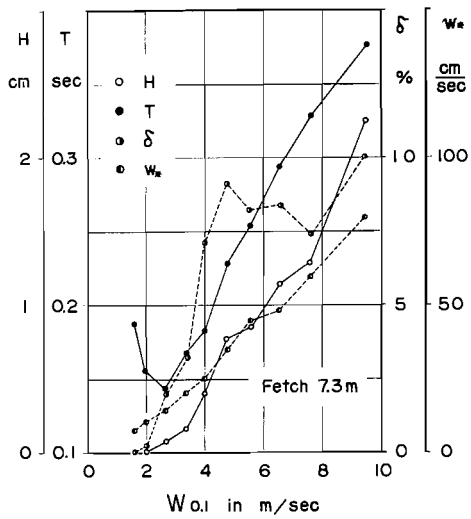


Fig. 16. An example of development of some wave characteristics and friction velocity.

In Fig. 16 some wave characteristics and the friction velocity at the fetch of 7.3 m are shown against the wind velocity $W_{0.1}$, both on a linear scale. Here it is important to note that with the increase of wind velocity the average wave period at first decreases and then increases, in other words, there is a minimum wave period in the course of development of initial wavelets. This interesting fact was observed at every fetch during our second experiment. We call the stages of initial wavelet before and after this critical state the earlier stage and the later stage of initial wavelet respectively. The corresponding critical value of $w_*H/\nu_a$ is roughly estimated to be about 6, though the values obtained from the different fetches are not in full agreement with one another. From the practical point of view one may consider it as the critical value of wave generation, since the average wave height and the steepness are roughly 0.8 mm and 2% respectively and one can easily and definitely observe waves. Although the cause of the existence of minimum wave period is not known, a possible explanation will be discussed in Section 4.3.

### 4.2. Transition to sea wave and empirical law of initial wavelet

The initial wavelets are recognized as roughness elements, while further developed ocean waves cannot possibly be regarded as the roughness elements themselves. In reality, the initial wavelets have no such $\beta-\delta$ dependence as has been found in the ocean waves by Sverdrup-Munk. This is shown in Fig. 17. Obviously the relation between steepness $\delta$ and wave age $\beta'=c/w_*$ for initial wavelets is not universal but depends upon the fetch. For comparison the Sverdrup-Munk's curve is shown by a broken line after the consideration that $w_*^2=2.6\times10^{-3}W_{10}^2$. The initial wavelets are quite different from further developed waves in

character. There must be a transition between them.

The fetch graph is useful in investigating this transition. Taking the quantity $gF/w_*^2$ as the abscissa and $gH/w_*^2$ the ordinate, both on a logarithmic scale, we obtain Fig. 18 from all of our data in the second experiment. With the increase of wind velocity our data at each fetch move upwards from the lower right part of the figure and converge to a line. This convergence seems to indicate the transition from the initial wavelet to the further developed wave which we name 'sea wave', because it is widely accepted that what is called 'sea' is represented by a line on the fetch graph. Bretschneider's curve is shown by way of comparison by a broken line in the same figure after

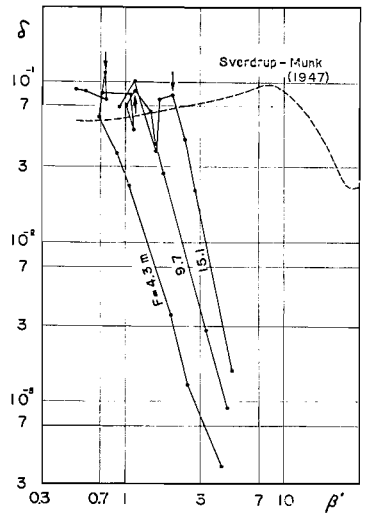


Fig. 17. Relation between wave steepness and wave age.

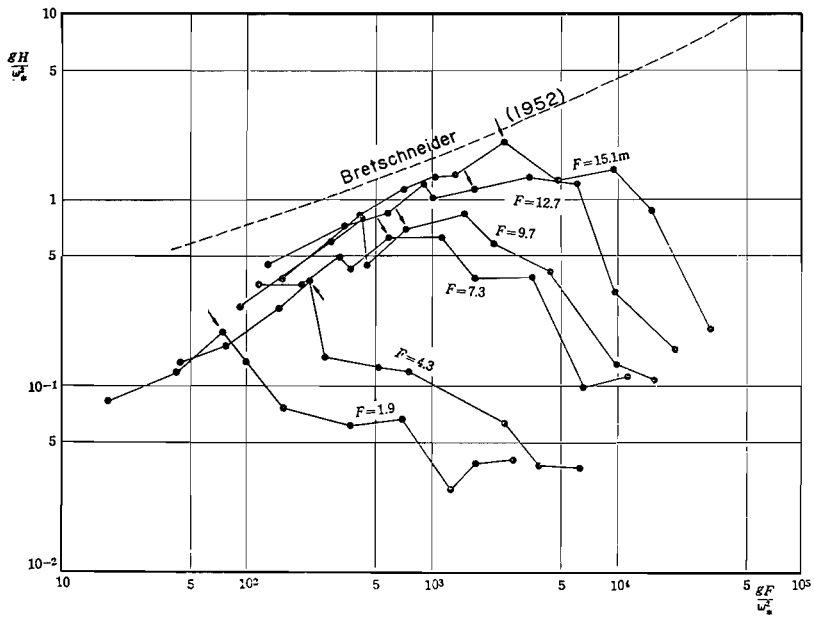


Fig. 18. Fetch graph.

the same consideration as before.

If we assume that the transition occurs at the points shown by arrows in the same figure i.e. runs 8, 17, 6, 16, 5 and 15 in order of fetch, we find that their values of $w_*H/\nu_a$ generally agree. This is shown by arrows at the right part of Fig. 14 and 15. The reasonable value for this transition is estimated at about 200.

Further it must be noted here that these critical data are at the same time associated with the first maximum of steepness at each fetch with the exception of the fetch of 12.7 m, as shown by arrows in Fig. 17. This is suggestive. We have at first supposed that the transition to sea wave is probably due to the breaking process of waves. The visual observation, however, has not always given positive impression. The alternative interpretation of this point will be presented in the next section. Here we must notice that the change in the appearance of the wave surface, from relatively smooth to very rough, occurs after the transition to sea wave. This change, however, seems to be related not to the above transition but to the wind velocity itself. Its wind velocity is about $\overline{W}=7.5$ m/sec.

As previously stated, the initial wavelet has no $\beta-\delta$ dependence. By what can it be replaced? We have succeeded to find it after various trials. the universal relationship of the initial wavelet exists between the quantities $w_*H/\nu_a$ and $w_*L/\nu_a$. This relation is presented in Fig. 19. The ar-

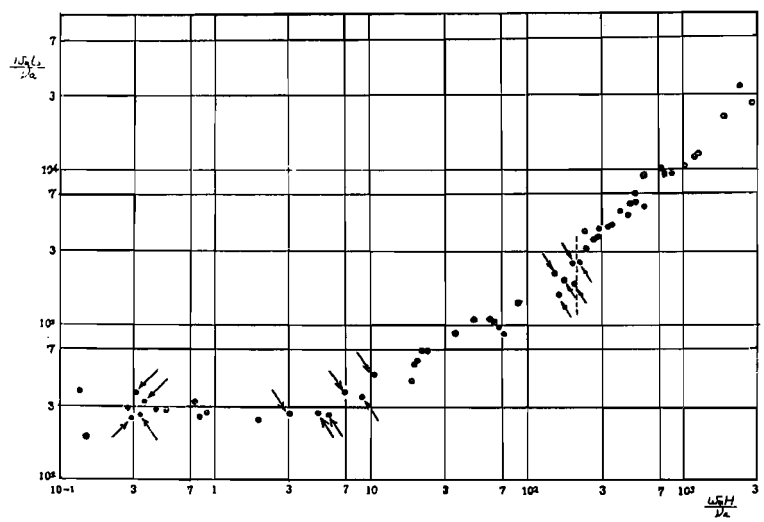

Fig. 19. Empirical law of initial wavelet.

rows at the left and right parts of this figure correspond to those in Fig. 14 and 15 and indicate the generation of initial wavelet and the transition to sea wave respectively. The arrows in the central part represent the data with the minimum wave periods of which mention is made in Section 4.1. It must be noted here that the value of $w_*L/\nu_a$ remains nearly constant in the earlier stage of initial wavelet.

This relation is a very important result of our experiment in the meaning that it offers a key to elucidate the mechanism of the generation and growth of initial wavelets. Though the author, at present, is unable to formulate a consistent theory of initial wavelets, it may be worthwhile to discuss further some empirical evidence on the mechanism of the development of initial wavelets.

### 4.3. Sheltering effect of initial wavelet and energy process of wave growth

As described in Section 4.1, there is a mutual action between air flow and initial wavelet. This concept can be fixed after H. Jeffreys (1925, 1926) by introducing the pressure fluctuation $\Delta p$ along wave surfaces due to the sheltering effect of initial wavelet. The shearing stress at water surface $\tau_0$ and the mean rate of energy transfer from air to wave $R_N$ can be expressed as follows in terms of the quantity $\Delta p$

$$\tau_0=\tau_s+\Delta\tau \quad \text{and} \quad \Delta\tau=\frac{1}{L_0}\int_0^L \Delta p\frac{\partial\zeta}{\partial x}dx, \qquad \cdots\cdots(4.8)$$

$$R_N=\frac{1}{L}\int_0^L \Delta p\cdot w_0 dx, \qquad \cdots\cdots(4.9)$$

where $\zeta$ is the elevation of water surface, $w_0$ the vertical velocity of water particle at the surface, $\tau_s$ the skin friction, and $\Delta\tau$ the form drag due to the initial wavelet. The suffix $N$ means that the energy transfer is due to the normal stress. In general, the integral limit $L$ is taken as sufficiently large.

If we further assume a simple harmonic surface wave

$$\zeta=\frac{H}{2}\sin\frac{2\pi}{L}(x-Ct), \quad w_0=\pi C\frac{H}{L}\cos\frac{2\pi}{L}(x-Ct), \qquad \cdots\cdots(4.10)$$

we may easily obtain the following expression

$$R_N=C\cdot\Delta\tau=C(\tau_0-\tau_s). \qquad \cdots\cdots(4.11)$$

This relation makes it possible to estimate the energy transfer $R_N$ from

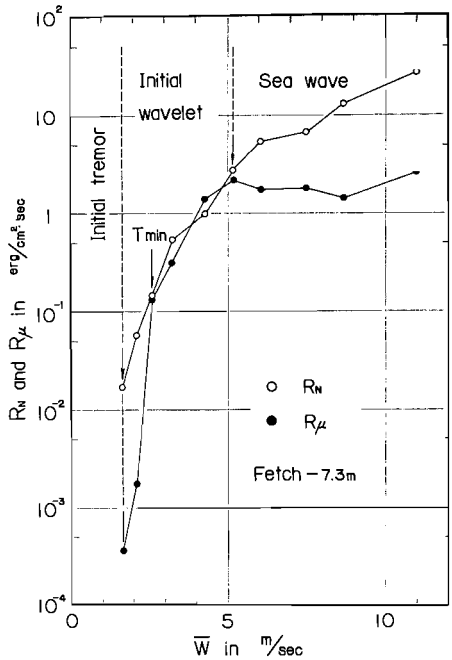


Fig. 20. Comparison between energy transfer to wave and dissipation of wave energy.

our observed data of surface stress, since the assumption of simple harmonic wave (4.10) may be allowed for the initial wavelet which is considered to have a narrow band width. In Fig. 20 an example of such an estimation of $R_N$ is shown in comparision with the dissipation of wave energy $R_\mu$. Here $R_\mu$ is calculated by the formula

$$R_\mu = 4\pi^3 \mu_w \frac{C^2 H^2}{L^3} = 2\pi^2 g \mu_w \delta^2 \left\{1 + \left(\frac{L_0}{L}\right)^2\right\}, \quad (4.12)$$

where $L_0 = 2\pi\sqrt{S/\rho_w g} \simeq 1.7$ cm is the well-known wave length of the wave having a minimum phase velocity. As seen in the figure, the dissipation $R_\mu$ rapidly becomes comparable to the income $R_N$ at the end of the earlier stage of initial wavelet, and again becomes considerably smaller than $R_N$ after the transition to sea wave. Since the assumption (4.10) may not be allowed for the regime of sea wave, our estimation of $R_N$ in this regime is somewhat uncertain, but the general character mentioned above might not be altered. Probably the mechanism of the initiation of the later stage of initial wavelet is the 'sorting' of the spectral component waves resulting from the saturation of shorter waves due to larger dissipation of them.

In connection with this, it must be noted that the relation (4.8) gives a possibility to infer the nature of pressure fluctuation $\Delta p$. If we again assume a simple harmonic wave (4.10), and further assume after Jeffreys that

$$\Delta p = \rho_a s (W - C)^2 \frac{\partial \zeta}{\partial x}, \quad \cdots\cdots\cdots\cdots\cdots (4.13)$$

and write that

$$\gamma^2=\frac{\tau_0}{\rho_a W^2}=\frac{w_*^2}{W^2},\quad \gamma_s^2=\frac{\tau_s}{\rho_a W^2}\quad\text{and}\quad \Delta\gamma^2=\frac{\Delta\tau}{\rho_a W^2},\quad\cdots\cdots(4.14)$$

we shall obtain the following expression from the equation (4.8)

$$\Delta\gamma^2=\gamma^2-\gamma_s^2=\frac{\pi^2}{2}s\delta^2\left(1-\frac{C}{W}\right)^2\quad\cdots\cdots\cdots\cdots\cdots\cdots(4.15)$$

where $s$ is called the 'sheltering coefficient'. By this relation we can infer the nature of sheltering coefficient $s$ from our observed data as far as the assumption of simple harmonic wave (4.10) is valid.

There is, however, a fundamental difficulty. We cannot estimate the value of skin friction $\tau_s$ so definitely without further information on it. With using the values of wind velocity at 10 m above water surface $W_{10}$ which are extrapolated by the formula (3.2), we estimate the values of $\gamma_s^2$ by the formula (3.1). This procedure was taken only for convenience, but the similar trial using the values of wind velocity at 10 cm above water surface proved that both results are, as a whole, identical in character.

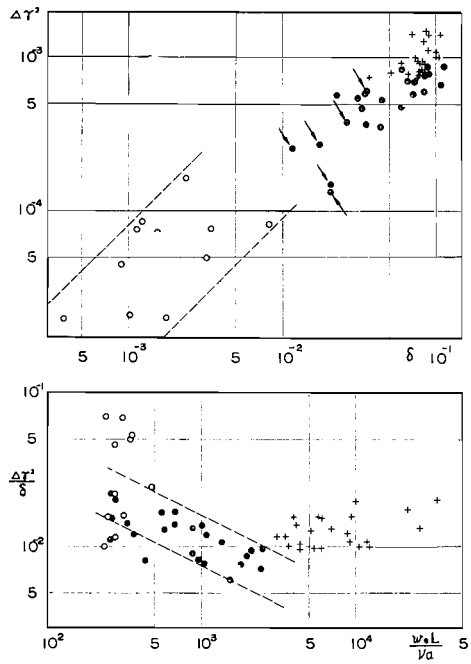


Fig. 21. Relation between $\Delta\gamma^2$ and $\delta$ and $w_*L/\nu_a$.

The upper figure of Fig. 21 is the result. In this figure the blank circles, solid circles, and cross marks are our data obtained from earlier stage, later stage of initial wavelet, and sea wave respectively. The arrows indicate the data with minimum wave periods. Obviously $\Delta\gamma^2$ is not proportional to $\delta^2$, therefore the sheltering coefficient $s$ is not regarded as a constant. $\Delta\gamma^2$ seems to be roughly proportional to $\delta^{1/2}$ as a whole, but the blank circles whose outer edges are shown by broken lines are proportional to $\delta$. This suggests that the sheltering coefficient depends not only on $\delta$ but also on $w_*L/\nu_a$, because the relation between $\Delta\gamma^2$ and $\delta$ seems to be altered by

the loss of the nature that the value of $w_*L/\nu_a$ remains constant.

From this point of view we can infer that

$$\Delta\gamma^2 \propto \frac{\delta}{\sqrt{\frac{w_*L}{\nu_a}}} \quad \text{and accordingly} \quad s \propto \frac{1}{\delta\sqrt{\frac{w_*L}{\nu_a}}}, \qquad \cdots\cdots(4.16)$$

as can be seen from the lower figure of Fig. 21. It is reasonable that the sheltering effect diminishes when the wave length increases against the thickness of laminar sub-layer which is proportional to $\nu_a/w_*$ in a rough measure. Thus, the energy transfer to wave $R_N$ is expressed as

$$R_N \propto \frac{C\delta}{\sqrt{\frac{w_*L}{\nu_a}}}(W-C)^2 \qquad \cdots\cdots(4.17)$$

If we assume that the relation (4.17) is also valid for each spectral component wave, we are able to see that the wave length at which the wave height takes a maximum value increases at a fixed fetch point with the increase of wind velocity owing to the energy dissipation of waves due to the viscosity. This cannot be given at all in the case of the sheltering coefficient dependent on the steepness $\delta$ only, considering that $w_*^2=(\tau_s+\Delta\tau)/\rho_a=(\gamma_s^2+\Delta\gamma^2)W^2$ and $\tau_s \propto W^{7/4}$ and assuming the relation

$$\frac{d}{dx}(G\cdot E)=R_N-R_\mu, \qquad \cdots\cdots(4.18)$$

where the group velocity $G$ and the mean total energy $E$ are defined as

$$G=C\left\{\frac{1}{2}+\frac{(L_0/L)^2}{1+(L_0/L)^2}\right\} \quad \text{and} \quad E=\frac{\pi\rho_m}{4}\frac{C^2H^2}{L} \qquad \cdots\cdots(4.19)$$

Further, since it is considered that, near and after the transition to sea wave, $w_*^2 \simeq \Delta\tau/\rho_a=\Delta\gamma^2\cdot W^2$ for component waves near the peak of the spectrum, $R_N$ takes the form of $\delta^{4/5}\cdot L^{1/10}$ in the range of wave length of our interest. With this consideration, the possibility that longer waves predominate without the restriction of viscosity in the regime of sea wave can be seen as well as in the case of the sheltering coefficient proportional to $\delta^\alpha$ in which $-2<\alpha<0$, assuming that the steepness cannot grow beyond the maximum value of about 0.1. Here it must be remembered what was mentioned in the last part of Section 4.2. The restriction that the maximum value of steepness $\delta$ is about 0.1 does not always mean the breaking of waves. Probably the full mechanism of the transition to sea wave can be

pursued in the possibility of rather continuous energy transfer to longer waves due to the non-linear interaction between the spectral component waves. This presents a very interesting future problem. The energy transfer to water current or to turbulent eddies also may be considered.

The present spectral form of energy income (4.17) is not always sufficient to explain the first decrease of wave period with the increase of wind velocity as described in the preceding section. It seems hobeful, hewever, that it may be interpreted in the future more detailed examinations along this line of research that the sheltering coefficient depends not only on $\delta$ but also $w_*L/\nu_a$. Probably the precise spectral form of the sheltering coefficient is more complicated. There is also the possibility that it depends on the fetch.

What the author would conclude in this section is that the nature of energy transfer to waves due to the sheltering effect is more favourable for the accumulation of shorter waves with the increase of wind velocity, and that the initiation of later stage of initial wavelet and of sea wave result from the saturation of shorter waves, which occurs owing to the energy dissipation due to the viscosity, and owing to the energy transfer to longer waves, to water corrents, and to turbulent eddies due to the non-linear interaction respectively.

### 4.4. Quantity $gz_0/w_*^2$ and friction factor

If we reformulate the equation (4.18) to the non-dimensional form with respect to the quantities $w_*H/\nu_a$ and $w_*L/\nu_a$, we shall be able to recognize the need of introducing a new quantity $w^3{}_*/g\nu_a$. It can be rewritten as follows

$$\frac{w_*{}^3}{g\nu_a}=\frac{w_*z_0/\nu_a}{gz_0/w_*{}^2} \qquad \cdots\cdots\cdots\cdots\cdots\cdots(4.20)$$

The first quantity $w_*z_0/\nu_a$ is a function of $w_*H/\nu_a$, as is shown by the equation (4.6). But the second quantity $gz_0/w_*{}^2$ proves to be a new independent one, as can be seen in the upper figure of Fig. 22. It depends not upon the quantity $w_*H/\nu_a$ but upon the fetch $F$ in the region of initial wavelet. The lower figure shows its dependence on the fetch. Each blank circle is the mean value of $gz_0/w_*{}^2$ in the regime of initial wavelet at each fetch of observation, and the broken line represents the following equation

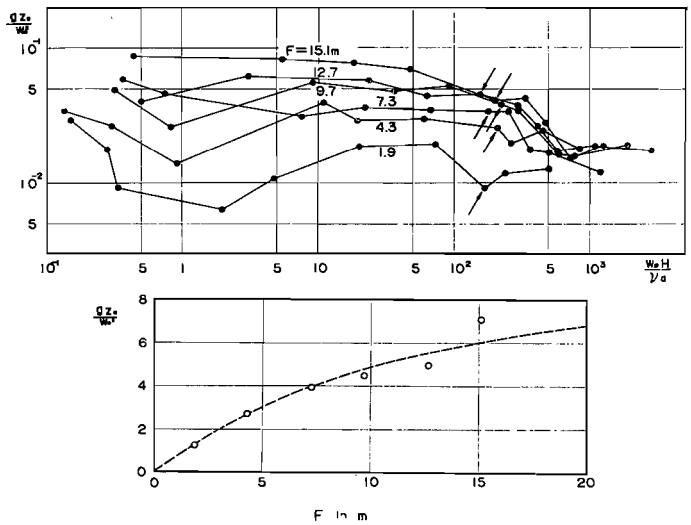


Fig. 22. Behaviour of $gz_0/w_*^2$.

$$\frac{gz_0}{w_*^2}=8.0\times10^{-2}\{1-e^{-9.2\times10^{-2}F}\} \quad (F \text{ in } m) \quad \cdots\cdots\cdots\cdots(4.21)$$

It is very interesting that the dependence of initial wavelet on the fetch is explicitly and essentially expressed by this quantity and that this quantity converges to a constant value independent of the fetch with the transition to sea wave, as seen in the same figure. The constancy of this value in the ocean at sufficiently high wind speed has been pointed out by H. Charnock (1955) and also by T. H. Ellison (1956), although the numerical values are quite different from ours in the region of sea wave. F. Ursell (1956) and T. H. Ellison (1956) have pointed out that it is the only dimensionally correct relation when the wind is fully rough. It is, however, rather astonishing that at a fixed fetch point the constancy of this value also holds in the regime of initial wavelet where the wind is not fully rough but transitional. These facts seem to imply an important physical significance, but its nature is not yet clear.

In connection with this, another practically important quantity must be mentioned. In the ocean the tangential stress $\tau_0$ exerted on the sea surface is usually assumed to be proportional to the square of wind velocity $W_{10}$ at 10 m above the sea surface and written by

$$\tau_0=\rho_a\gamma^2 W_{10}^2. \quad \cdots\cdots\cdots\cdots(4.22)$$

Here the non-dimentional proportional factor $\gamma^2$ is called 'friction factor' We can calculate the values of $\gamma^2$ in the following form

$$\gamma^2=\frac{w_*{}^2}{W_{10}{}^2}, \qquad \cdots\cdots\cdots\cdots\cdots\cdots(4.23)$$

using the values of wind velocity at 10 m above water surface which are extraporated by the formula (3.2) from our data.

The upper figure of Fig. 23 is the result, in which our data are shown by different marks indicating different fetches. The broken line corresponds to the wind along smooth surfaces and it is what has been used to estimate the values of $\gamma_s^2$ in the previous Section 4.3. Obviously our data depend upon the fetch, but this dependence seems to become smaller with the increase of fetch. It should be so, since our calculation is equi-

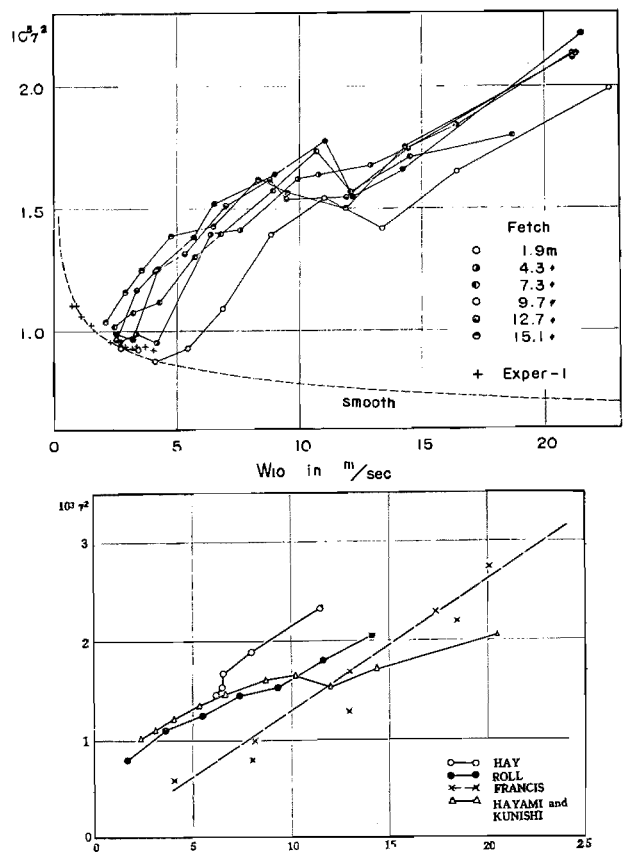


Fig. 23. Friction factor.

valent to the following one

$$\frac{1}{\gamma}=\frac{W_{10}}{w_*}=5.75\log\frac{10^3}{z_0}=5.75\left\{\log\frac{10^3 g}{w_*^2}-\log\frac{gz_0}{w_*^2}\right\}, \quad \cdots\cdots(4.24)$$

and $gz_0/w_*^2$ depends upon the fetch as stated before.

As a whole, the friction factor $\gamma^2$ increases with the wind velocity. This general trend agrees with those of several authors shuch as H. U. Roll (1955) and J. S. Hay (1955), and the numerical value nearly agrees with Roll's in the range of wind velocity from 2 to 10 m/sec in which it increases from $0.9\times10^{-3}$ to $1.6\times10^{-3}$ These are shown in the lower figure of Fig. 23 in which each of our data shown by a triangular mark is the mean of four data at longer fetches to which roughly equal wind velocities are annexed.

As can be seen, our result remains nearly constant with a value of about $1.6\times10^{-3}$ near the wind velocity of 10 m/sec, and increases again at the wind velocity of about 12 m/sec. This increase corresponds to the change in the appearance of the 'wave' surface as described in Section 4.2. A similar tendency is also seen in the results of Roll, but the wind velocity at which $\gamma^2$ begins to increase is quite different from ours. This difference seems to be related to the difference in $gz_0/w_*^2$ between the open sea and the laboratory, but it is not completely clear.

## 5. Conclusion

Analysis of our experimental investigation conducted on the generation and growth of wind waves leads to the following conclusions.

1. There are at least three regimes in the course of generation and growth of wind waves. We call them initial tremor, initial wavelet, and sea wave in order of their appearance. The transitions between them are given by $w_*H/\nu_a\simeq0.3$ and 200.

2. There are two stages in the regime of initial wavelet. We call them earlier stage and later stage of initial wavelet in order of their appearance. The transition between them is characterized by a minimum wave period and is given by $w_*H/\nu_a\simeq6$.

3. The initial wavelets are recognized as roughness elements on the water surface. The nature of initial wavelt as roughness is similar to that of natural roughness, and the value of $n$ (the ratio of the roughness

parameter $z_0$ to the roughness height $k$ in the regime of fully rough wind) is about three times that in the case of a solid wall.

4. A universal relation by which the initial wavelets are governed exists between $w_*H/\nu_a$ and $w_*L/\nu_a$. In the earlier stage of initial wavelet the value of $w_*L/\nu_a$ remains nearly constant, while in the later stage $w_*L/\nu_a$ is nearly proportional to the square root of $w_*H/\nu_a$.

5. On the physical mechanism of the development of wind waves there is empirical evidence to support the conjecture that the sheltering coefficient depends not only on $\delta$ but also on $w_*L/\nu_a$, and the dissipation of wave energy becomes comparable to the energy transfer to wave in the later stage of initial wavelet. These lead us to the conjecture that the increase of mean wave length with the increase of wind velocity is understood as the shift of the peak of wave spectrum toward longer wave length, resulting from the energy dissipation due to viscosity, and the energy transfer to longer waves due to non-linear interation between component waves.

6. The direct and essential dependence of initial wavelets on the fetch is borne by the quantity $gz_0/w_*^2$. This quantity becomes independent of the fetch and converges to a constant value with the transition to sea wave.

7. The friction factor $\gamma^2$, as a whole, increases with the wind velocity. It remains constant, however, near the wind velocity of 10 m/sec at 10 m above the water surface and its value is about $1.6\times10^{-3}$. It begins to increase again at about 12 m/sec. The beginning of this increase corresponds to the change in the appearance of the wave surface, from relatively smooth to very rough.

## Acknowledgements

The author wishes to express his heartfelt thanks to Prof. S. Hayami, Kyoto University, for his continuous advice and encouragement throughout the course of the present investigation. The author is also obliged to Mr. H. Higuchi, Mr. K. H. Yoshida and Mr. Y. Tani for their help in conducting experiments and in evaluating the data.

## References


Barber, N. F. and F. Ursell (1948): The generation and propagation of ocean waves and swell. Phil. Trans. Roy. Soc., 240, 527-560.

Bretschneider, C. L. (1952): The generation and decay of wind waves in deep water. Trans. A. G. U., 33, 381-389.

Bretschneider, C. L. (1959): Wave variability and wave spectra for wind generated gravity waves. Beach Erosion Bd. Techn. Mem., No. 118.

Charnock, H. (1955): Wind stress on a water surface. Quart. J. Roy. Meteorol. Soc., 81, 639.

Colebrook, C. F. (1939): Turbulent flow in pipes, with particular reference to the transition region between the smooth and rough pipe laws. Jour. Inst. Civil Engineers, 11, 133-156.

Darbyshire, J. (1952): The generation of waves by wind. Proc. Roy. Soc. A, 215, 299-328.

Darbyshire, J. (1955): An investigation of storm waves in the North Atlantic Ocean. Proc. Roy. Soc. A, 230, 560-569.

Darbyshire, J. (1956): An investigation into the generation of waves when the fetch of the wind is less than 100 miles. Quart. J. Roy. Meteorol. Soc., 82, 461-468.

Deacon, G. E. R. (1949): Recent studies of waves and swell. Ann. N. Y. Acad. Sci., 51, 475-482.

Ellison, T. H. (1956): Atmospheric turbulence. Surveys in mechanics, Cambridge Univ. Press, 400-430.

Eckart, C. (1953): The generation of wind waves over a water surface. J. Appl. Phys., 24, 1485-1494.

Hay, J. S. (1955): Some observations of air flow over the sea. Quart. J. Roy. Meteorol. Soc., 81, 307-319.

Hayami, S. and H. Kunishi (1959): A wind flume study on the generation of waves. Proc. Intern. Oceanog. Congr. (Preprints), 753-755.

Jeffreys, H. (1925): On the formation of water waves by wind. Proc. Roy. Soc. A, 107, 189-206.

Jeffreys, H. (1926): On the formation of water waves by wind (second paper). Proc. Roy. Soc. A, 110, 241-247.

Kawata, S., Y. Ōmori and K. Nishimura (1952): Characteristics of a theromocouple anemometer. Mem. Fac. Eng. Kyoto Univ., 14, 12-29.

Keulegan, G. H. (1951): Wind tides in small closed channels. Res. Nat. Bur. Stand., 46, 358-381.

Kunishi, H. (1957): Studies on wind waves by wind flume experiments (1) (in Japanese). Ann. Disas. Prev. Res. Inst., 1, 119-127.

Kunishi, H. (1959): On design of resistive wave meter (in Japanese). Ann. Disas. Prev. Res. Inst., 3, 65-73.

Lock, R. C. (1954): Hydrodynamic stability of the flow in the laminar boundary layer between parallel streams. Proc. Camb. Phil. Soc., 50, 105-124.

Longuet-Higgins, M. S. (1952): On the statistical distribution of the heights of sea waves. J. Mar. Res., 11, 245-266.

Miles, J. W. (1957): On the generation of surface waves by shear flows. J. Fluid Mech., 3, 185-204.

Munk, W. H. (1947): A critical wind speed for air-sea boundary processes. J. Mar. Res., 6, 203-218.

Neumann, G. (1952a): Über die komplexe Natur des Seeganges, I Teil. Dtsch. Hydrogr. Z., 5, 95-110.

Neumann, G. (1952b): Über die komplexe Natur des Seeganges, II Teil. Dtsch. Hydrogr. Z., 5, 252-277.

Neumann, G. (1953a): Notes on the generation and growth of ocean waves under wind action. Proc. 3rd Conference on Coastal Engineering, 77-85.

Neumann, G. (1953b): On ocean wave spectra and a new method of forecasting wind-generated sea. Beach Erosion Bd. Techn. Mem., No. 43.

Nikuradse, J. (1933): Strömungsgesetze in rauhen Rohren, VDI Forschungsheft, No. 361.

Paeschke, W. (1937) Experimentelle Untersuchungen zum Rauhigkeits und Stabilitäts problem in der bodennahen Luftschicht. Beitr. Phys. fr. Atm., 24, 163-189.

Phillips, O. M. (1957): On the generation of waves by turbulent wind. J. Fluid Mech., 2, 417-445.

Phillips, O. M. (1958): The equilibrium range in the spectrum of wind generated waves. J. Fluid Mech., 4, 426-434.

Pierson, W. J., Jr. (1952): A unified mathematical theory for the analysis, propagation, and refraction of storm-generated ocean surface waves, Part I and II. Res. Div. Coll. Engineering. N. Y. Univ.

Pierson, W. J., Jr., G. Neumann and R. W. James (1955): Practical Methods for observing and forecasting ocean waves by means of wave spectra and statistics. H. O. Pub., No. 603.

Roll, H. U. (1951): Neue Messungen von Wasserwellen durch Wind. Ann. Met. Hamburg, 1, 139-151.

Roll, H. U. (1955): Discussion on air flow over the sea. Quart J. Roy. Meteorol. Soc., 81, 631-632.

Roll, H. U. und G. Fischer (1956): Eine kritische Bemerkung zum Neumann-Spektrum des Seeganges. Dtsch. Hydrogr. Z., 9, 9-14.

Sibul, O. (1955): Water surface roughness and wind shear stress in a laboratory wind-wave channel. Beach Erosion Bd. Techn. Mem., No. 74.

Sverdrup, H. U. and W. H. Munk (1946): Empirical and theoretical relation between wind, sea, and swell. Trans. A.G.U., 27, 823-827.

Sverdrup, H. U. and W. H. Munk (1947): Wind, sea and swell; theory of relations for forecasting. H.O. Pub. No. 601.

Ursell, F. (1956): Wave generation by wind. Surveys in mechanics, Cambridge Univ. Press, 216-249.

van Dorn, W. G. (1953): Wind stress on an artificial pond. J. Mar. Res., 12, 249-276.

Wüst, W. (1949): Beitrag zur Entstehung von Wasserwellen durch Wind. Z. angew. Math. Mech., 29, 239-252.

## Publications of the Disaster Prevention Research Institute

The Disaster Prevention Research Institute publishes reports of the research results in the form of bulletins. Publications not out of print may be obtained free of charge upon request to the Director, Disaster Prevention Research Institute, Kyoto University, Kyoto, Japan.

### Bulletins :

No. 1 On the Propagation of Flood Waves by Shoitiro Hayami, 1951.

No. 2 On the Effect of Sand Storm in Controlling the Mouth of the Kiku River by Tojiro Ishihara and Yuichi Iwagaki, 1952.

No. 3 Observation of Tidal Strain of the Earth (Part I) by Kenzo Sassa, Izuo Ozawa and Soji Yoshikawa. And Observation of Tidal Strain of the Earth by the Extensometer (Part II) by Izuo Ozawa, 1952.

No. 4 Earthquake Damages and Elastic Properties of the Ground by Ryo Tanabashi and Hatsuo Ishizaki, 1953.

No. 5 Some Studies on Beach Erosions by Shoitiro Hayami, Tojiro Ishihara and Yuichi Iwagaki, 1953.

No. 6 Study on Some Phenomena Foretelling the Occurrence of Destructive Earthquakes by Eiichi Nishimura, 1953.

No. 7 Vibration Problems of Skyscraper. Destructive Element of Seismic Waves for Structures by Ryo Tanabashi, Takuzi Kobori and Kiyoshi Kaneta, 1954.

No. 8 Studies on the Failure and the Settlement of Foundations by Sakurō Murayama, 1954.

No. 9 Experimental Studies on Meteorological Tsunamis Traveling up the Rivers and Canals in Osaka City by Shoitiro Hayami, Katsumasa Yano, Shohei Adachi and Hideaki Kunishi, 1955.

No.10 Fundamental Studies on the Runoff Analysis by Characteristics by Yuichi Iwagaki, 1955.

No.11 Fundamental Considerations on the Earthquake Resistant Properties of the Earth Dam by Motohiro Hatanaka, 1955.

No.12 The Effect of the Moisture Content on the Strength of an Alluvial Clay by Sakurō Murayama, Kōichi Akai and Tōru Shibata, 1955.

No.13 On Phenomena Forerunning Earthquakes by Kenzo Sassa and Eiichi Nishimura, 1956.

No.14 A Theoretical Study on Differential Settlements of Structures by Yoshitsura Yokoo and Kunio Yamagata, 1956.

No.15 Study on Elastic Strain of the Ground in Earth Tides by Izuo Ozawa, 1957.

No.16 Consideration on the Mechanism of Structural Cracking of Reinforced Concrete Buildings Due to Concrete Shrinkage by Yoshitsura Yokoo and S. Tsunoda. 1957.

No.17 On the Stress Analysis and the Stability Computation of Earth Embankments by Kōichi Akai, 1957.

No.18 On the Numerical Solutions of Harmonic, Biharmonic and Similar Equations by the Difference Method Not through Successive Approximations by Hatsuo Ishizaki, 1957.

No.19 On the Application of the Unit Hydrograph Method to Runoff Analysis for Rivers in Japan by Tojiro Ishihara and Akiharu Kanamaru, 1958.

No.20 Analysis of Statically Indeterminate Structures in the Ultimate State by Ryo Tanabashi, 1958.

No.21 The Propagation of Waves near Explosion and Fracture of Rock (I) by Soji Yoshikawa, 1958.

No.22 On the Second Volcanic Micro-Tremor at the Volcano Aso by Michiyasu Shima, 1958.

No.23 On the Observation of the Crustal Deformation and Meteorological Effect on It at Ide Observatory and On the Crustal Deformation Due to Full Water and Accumulating Sand in the Sabo-Dam by Michio Takada, 1958.

No.24 On the Character of Seepage Water and Their Effect on the Stability of Earth Embankments by Kōichi Akai, 1958.

No.25 On the Thermoelasticity in the Semi-infinite Elastic Soid by Michiyasu Shima, 1958.

No 26 On the Rheological Characters of Clay (Part 1) by Sakurō Murayama and Tōru Shibata, 1958.

No.27 On the Observing Instruments and Tele-metrical Devices of Extensometers and Tiltmeters at Ide Observatory and On the Crustal Strain Accompanied by a Great Earthquake by Michio Takada, 1959.

No.28 On the Sensitivity of Clay by Shinichi Yamaguchi, 1959.

No.29 An Analysis of the Stable Cross Section of a Stream Channel by Yuichi Iwagaki and Yoshito Tsuchiya, 1959.

No.30 Variations of Wind Pressure against Structures in the Event of Typhoons by Hatsuo Ishizaki, 1959.

No.31 On the Possibility of the Metallic Transition of MgO Crystal at the Boundary of the Earth's Core by Tatsuhiko Wada, 1960.

No.32 Variation of the Elastic Wave Velocities of Rocks in the Process of Deformation and Fracture under High Pressure by Shogo Matsushima, 1960.

No.33 Basic Studies on Hydraulic Performances of Overflow Spillways and Diversion Weirs by Tojiro Ishihara, Yoshiaki Iwasa and Kazune Ihda, 1960.

No.34 Volcanic Micro-tremors at the Volcano Aso by Michiyasu Shima, 1960.

No.35 On the Safety of Structures Against Earthquakes by Ryo Tanabashi, 1960.

No.36 On the Flow and Fracture of Igneous Rocks and On the Deformation and Fracture of Granite under High Confining Pressure by Shogo Matsushima, 1960.

No.37 On the physical properties within the B-layer deduced from olivine-model and on the possibility of polymorphic transition from olivine to spinel at the 20° Discontinuity by Tatsuhiko Wada, 1960.

No.38 On Origins of the Region C and the Core of the Earth ——Ionic-Intermetallic-Metallic Transition Hypothesis—— by Tatsuhiko Wada, 1960.

No.39 Crustal Stucture in Wakayama District as Deduced from Local and Near Earthquake Observations by Takeshi Mikumo, 1960.

No.40 Earthquake Resistance of Traditional Japanese Wooden Structures by Ryo Tanabashi, 1960.

No.41 Analysis With an Application to Aseismic Design of Bridge Piers by Hisao Goto and Kiyoshi Kaneta, 1960.

No.42 Tilting Motion of the Ground as Related to the Volcanic Activity of Mt. Aso and Micro-Process of the Tilting Motion of Ground and Structure by Yoshiro Itō, 1961.

No.43 On the Strength Distribution of the Earth's Crust and the Upper Mantle, and

the Distribution of the Great Earthquakes with Depth by Shogo Matsushima, 1961

No.44 Observational Study on Microseisms (Part 1) by Kennosuke Okano, 1961.

No.45 On the Diffraction of Elastic Plane Pulses by the Crack of a Half Plane by Michiyasu Shima, 1961.

No.46 On the Observations of the Earth Tide by Means of Extensometers in Horizontal Components by Izuo Ozawa, 1961.

No.47 Observational Study on Microseisms (Part 2) by Kennosuke Okano, 1961.

No.48 On the Crustal Movement Accompanying with the Recent Activity on the Volcano Sakurajima (Part 1) by Keizo Yoshikawa, 1961.

No.49 The Ground Motion Near Explosion by Soji Yoshikawa, 1961.

No.50 On the Crustal Movement Accompanying with the Recent Activity of the Volcano Sakurajima (Part 2) by Keizo Yoshikawa, 1961.

No.51 Study on Geomagnetic Variation of Telluric Origin Part 1 by Junichiro Miyakoshi, 1962.

No.52 Considerations on the Vibrational Behaviors of Earth Dams by Hatsuo Ishizaki and Naotaka Hatakeyama, 1962.

No.53 Some Problems on Time Change of Gravity (Parts 1 and 2) by Ichiro Nakagawa, 1962.

No.54 Nature of the Volcanic Micro-Tremors at the Volcano Aso, Part 1. Observation of a New Type of Long-Period Micro-Tremors by Long-Period Seismograph by Kosuke Kamo, 1962.

No.55 Nature of the Volcanic Micro-Tremors at the Volcano Aso, Part 2. Some Natures of the Volcanic Micro-Tremors of the 1st kind at the Volcano Aso by Kosuke Kamo, 1962.

No.56 Nonlinear Torsional Vibration of Structures due to an Earthquake by Ryo Tanabashi, Takuji Kobori and Kiyoshi Kaneta, 1962.

No.57 Some Problems on Time Change of Gravity (Parts 3, 4 and 5) by Ichiro Nakagawa, 1962.

No.58 A Rotational Strain Seismometer by Hikaru Watanabe, 1962.

No.59 Hydraulic Model Experiment Involving Tidal Motion (Parts 1, 2, 3 and 4) by Haruo Higuchi, 1963.

No.60 The Effect of Surface Temperature on the Crustal Deformations by Shokichi Nakano, 1963.

No.61 An Experimental Study on the Generation and Growth of Wind Waves by Hideaki Kunishi, 1963.

Bulletin No. 61 Published March, 1963

昭和 38 年 3 月 16 日 印刷
昭和 38 年 3 月 20 日 発行
編輯兼
発行者 京都大学防災研究所
印刷者 山代多三郎
京都市上京区寺之内通小川西入
印刷所 山代印刷株式会社